Metformin preconditioning protects against myocardial stunning and preserves mitochondrial dynamics and protein translation in a mouse model of cardiac arrest

Cody A. Rutledge MD PhD[1], Claudia Lagranha PhD[1], Takuto Chiba PhD[2,3], Kevin Redding MS[1], Donna B. Stolz PhD[4], Eric Goetzman PhD[2], Sunder Sims-Lucas PhD[2,3], Brett A. Kaufman PhD[1]

1. Division of Cardiology, Vascular Medicine Institute, Department of Medicine, University of Pittsburgh, Pittsburgh, PA, USA

2. Rangos Research Center, Children's Hospital of Pittsburgh, University of Pittsburgh, Pittsburgh, PA, USA

3. Division of Nephrology, Department of Pediatrics, University of Pittsburgh School, Pittsburgh, PA, USA

4. Department of Cell Biology, University of Pittsburgh, Pittsburgh, PA, USA

Running Head: Metformin therapy protects against cardiac arrest

Corresponding Author:

Brett A. Kaufman

200 Lothrop Street

BST E1241

Pittsburgh, PA 15261

1-412-624-8644

bkauf@pitt.edu

Abstract

Cardiac arrest (CA) causes high mortality due to multi-system organ damage attributable to ischemia-reperfusion injury. Recent work in our group found that among diabetic patients who experienced cardiac arrest, those taking metformin had less evidence of cardiac and renal damage after cardiac arrest when compared to those not taking metformin. To investigate the potential for metformin to impact cardiac arrest outcomes, the current study investigates metformin interventions on cardiac and renal outcomes in a non-diabetic CA mouse model. We found that two weeks of metformin pretreatment protects against reduced ejection fraction and reduces kidney ischemia-reperfusion injury at 24 hours post-arrest. This cardiac and renal protection depends on AMPK signaling, as demonstrated by outcomes in mice pretreated with the AMPK activator AICAR or metformin plus the AMPK inhibitor compound C.

At this 24-hour time point, gene expression analysis showed that metformin pretreatment caused changes supporting autophagy, antioxidant response, and protein translation. Further investigation found associated improvements in mitochondrial structure and markers of autophagy. Notably, Western analysis indicated that protein synthesis was preserved in arrest hearts of animals pretreated with metformin. The AMPK activation-mediated protection of protein synthesis was also demonstrated in a hypoxia/reoxygenation cell culture model. Despite the positive impacts of pretreatment *in vivo* and *in vitro*, metformin did not preserve ejection fraction when deployed at resuscitation. Taken together, we propose that metformin's *in vivo* cardiac preservation occurs through AMPK activation, requires adaptation before arrest, and is associated with preserved protein translation.

46 **Introduction**

47 Cardiac arrest (CA) refers to the abrupt cessation of cardiac function and affects over 600,000 patients
48 annually in the United States (1,2). Patients with return of spontaneous circulation (ROSC) after CA
49 experience systemic ischemia-reperfusion injury, typically resulting in multi-system organ damage.
50 Common findings include cardiogenic shock, acute renal failure, liver damage, and neurologic
51 dysfunction (3–5). Previous observational studies in cardiac arrest patients have shown that low cardiac
52 ejection fraction (EF) (6) and reduced kidney function (7,8) after arrest are predictors of increased
53 mortality. Despite the prevalence of CA, no pharmacologic therapy has been shown to improve overall
54 survival.

55 A recent study by our group found that diabetic patients taking metformin had less evidence of cardiac
56 and renal damage after CA than diabetic patients on other treatments (9), suggesting that metformin
57 pretreatment may be beneficial to CA patients through an undefined mechanism. Metformin is an oral
58 antihyperglycemic agent used as a first-line agent for type 2 diabetes that enhances insulin sensitivity
59 and normalizes glucose and lipid homeostasis (10–13). Beyond its role in controlling diabetes,
60 metformin has demonstrated clinical benefit across a wide variety of pathologies, including decreased
61 mortality in the setting of coronary artery disease (14), congestive heart failure (15), acute kidney injury
62 (16), chronic kidney disease (15), septic shock (17,18), and major surgical procedures (19).
63 Cardiovascular studies suggest that improved outcomes occur independently of the glucose-lowering
64 effects of metformin and may instead be attributable to metformin's pleiotropic effects (20). In a
65 preclinical rat model of CA, metformin pretreatment improved neurologic outcomes and survival (21),
66 and similar protection was recently reported using metformin as a post-arrest therapy (22). However,
67 the mechanisms underlying this protection and the value of metformin as a rescue therapy after CA
68 remain unclear.

69 Several mechanisms beneficial to cardiovascular health have been implicated in metformin's effects,
70 including reduced oxidative stress, anti-apoptotic activities, JNK inhibition, complex I inhibition, and
71 AMP Kinase (AMPK) activation (21,23,24). AMPK activation is prevalent in the metformin literature and
72 AMPK activity is essential for survival after ischemic stress (25), but it is unclear whether AMPK activity is
73 the mediator of metformin-mediated protection in CA. Furthermore, it is not clear whether the adaptive
74 upregulation of AMPK during cardiac stress is optimal or whether further activation could even more
75 strongly impact recovery in cardiac injury models.

76 In this study, we sought to test metformin's potential benefit on heart and kidney protection after CA
77 and begin to assess the drivers of the effects witnessed clinically in our earlier diabetic patient study. We
78 evaluated cardiac and renal outcomes one day after CA in untreated sham (Sham), untreated arrest
79 (Arrest), metformin-pretreated sham (Sham+Met), and metformin pretreated arrest mice (Arrest+Met)
80 mice. Additionally, we tested the AMPK-dependence of metformin's effects by pretreating with the
81 AMPK activator 5-aminoimidazole-4-carboxamide-1-β-D-ribofuranoside (AICAR; Arrest+AICAR) instead
82 of metformin or by inhibition of AMPK via compound C given in the presence of metformin
83 (Arrest+Met+Comp C). We also evaluated a small cohort of mice with intravenous metformin as rescue
84 therapy. From the pretreatment group, we identified transcriptomic changes in metformin-treated
85 sham and arrest mice, and tested many of the pathways implicated by Western blot analysis or
86 confirmed changes in a cell model of hypoxia/reoxygenation (H/R).

87

Methods

Sudden Cardiac Arrest Model

Eight-week-old male and female C57BL/6J mice (Jackson Labs, Bar Harbor, ME, #000664) underwent cardiac arrest by delivery of potassium chloride (KCl) directly into the LV by percutaneous, ultrasound-guided needle injection (Figure 1) as previously described (26). Briefly, mice were anesthetized using vaporized isoflurane (Henry Schein, Melville, NY, #1182097) and endotracheally intubated, then mechanically ventilated (MiniVent, Harvard Apparatus, Holliston, MA, #73-0043) at a rate of 150 bpm and volume of 125 µL for females and 140 µL for males. Body temperature was maintained using a rectal temperature probe and heating pad (Indus Instruments, Webster, TX, #THM150). The chest was cleaned of hair using Nair and sterilized with betadine before the introduction of a 30-gauge needle into the LV under ultrasound guidance (Visual Sonics Vevo 3100 with Vevo LAB v 5.5.1 software, Toronto, Canada), followed by delivery of 40 µL of 0.5M KCl to induce asystole. The ventilator was stopped, and mice remained in asystole for a total of 8 minutes. 7.5 minutes after KCl dosing, 500 µL of 15 µg/mL epinephrine in saline (37 °C) was injected into the LV over approximately 30 seconds. At 8 minutes, the ventilator was restarted, and CPR was initiated by finger compression at about 300 bpm for 1-minute intervals. Electrocardiogram (ECG) was evaluated for return of sinus rhythm after each 1-minute interval. Animals not achieving ROSC by 3 minutes after CPR initiation were euthanized. Mice remained on ventilator support until spontaneous breathing frequency was greater than 60 times per minute. Sham mice received no KCl, but rather a single injection of epinephrine. After the procedure, all animals were placed in a recovery cage under a heat lamp.

Animal Treatment Groups

Treatment groups in the study were as follows: untreated sham (Sham), untreated cardiac arrest (Arrest), metformin-pretreated sham (Sham+Met), metformin-pretreated cardiac arrest (Arrest+Met), 5-aminoimidazole-4-carboxamide-1-beta-D-ribofuranoside (AICAR) pretreated cardiac arrest (Arrest+AICAR), metformin + compound c pretreated cardiac arrest (Arrest+Met+Comp C), and metformin rescue treatment cardiac arrest (Arrest+Rescue Metformin). Metformin pretreatment consisted of *ad libitum* access to metformin (Major Pharmaceuticals, Livonia, MI, #48152) in drinking water (1 mg/mL) for 14 days prior to procedure. AICAR pretreated mice were given IP injections of 500 mg/kg AICAR (Toronto Research Chemicals, Toronto, CA, #A611700) in saline every other day for 14 days prior to CA. Compound C pretreated mice were given 20 mg/kg IP injections of compound C (Cayman Chemical, Ann Arbor, MI, #11967) in saline daily for 14 days prior to arrest. Metformin rescue therapy was given as a single direct LV injection (1250 µg/kg) dissolved in saline along with 500 µL of 1 mg/mL epinephrine (Par Pharmaceutical, Chestnut Ridge, NY, #10977) at the time of resuscitation. Mice were randomly assigned to treatment groups. Male and female mice were used in all groups. All mouse studies were performed at the University of Pittsburgh in compliance with the National Institutes of Health Guidance for Care and Use of Experimental Animals. This protocol was approved by the University of Pittsburgh Animal Care and Use Committee (Protocol #18032212).

Echocardiography and Ultrasound

Immediately before arrest CA, mice were evaluated by transthoracic echocardiography using Vevo 3100 imaging systems (Visual Sonics) with a 40 MHz probe as previously described (27). Repeat echocardiography was performed one day after arrest under isoflurane anesthesia delivered by nose

129 cone. Heart rate was maintained between 400-500 bpm during imaging by adjusting isoflurane
130 concentration. B-mode images taken from the parasternal long-axis were captured, and LV EF was
131 calculated using modified Simpson's methods (28). A cohort of all groups was assessed for renal
132 perfusion after resuscitation. The ultrasound probe was oriented transversely across the abdomen at
133 the plane of the right kidney and monitored for renal artery blood flow by Doppler imaging. All image
134 analysis was performed by a blinded sonographer (Vevo Lab 5.5.1, Visual Sonics).

135 **Tissue and Serum Collection**

136 After euthanasia with isoflurane and cervical dislocation, mice underwent cardiac puncture to collect
137 blood by heparinized syringe. Blood was separated by centrifugation at 2,000 x g at 4°C for 10 minutes,
138 and the serum was flash frozen. These samples were evaluated for blood urea nitrogen (BUN) and
139 creatinine by the Kansas State Veterinary Diagnostic Laboratories (Manhattan, KS). Hearts from the mice
140 were excised, and LVs were isolated and flash frozen.

141 **Western Blot**

142 Frozen LV tissue was homogenized in lysis buffer containing a protease/phosphatase cocktail (Sigma-
143 Aldrich, St. Louis, MO, #11697498001) and normalized for protein content using a BCA assay (Life
144 Technologies, Carlsbad, CA, #23235). Samples were separated on NuPage 4-12% gradient SDS-PAGE gels
145 (ThermoFisher, Waltham, MA, #WG1403BOX) and iBlot transferred onto nitrocellulose membranes
146 (Invitrogen, #IB21001). Membranes were blocked in 5% milk (non-phosphorylated antibodies) or 5% BSA
147 (phosphorylated antibodies) for 1 hour and then incubated overnight at 4 °C with primary antibodies,
148 including, p-AMPK (Thr172, 1:1000, Cell Signaling, Danvers, MA, #2535), AMPK (1:1000, Cell Signaling,
149 #2532), GAPDH (1:5000, Millipore, St. Louis, MO, #AB2302), p62 (1:1000, Sigma-Aldrich, #P0067), LC3
150 (Invitrogen, 1:1000, PA1-16931), OxPhos Rodent Antibody Cocktail 1:5000 (ThermoFisher, #458099),
151 OPA1 (Invitrogen, 1:1000, PA5-57875), MFN2 (Invitrogen, 1:1000, #711803), p-DRP1 (Ser616, 1:1000,
152 Thermo, #PA5-64821), DRP1 (1:1000, Cell Signaling, #5391), p-S6 (Ser240/244, 1:1000, Cell Signaling,
153 #2215), S6 (1:1000, Cell Signaling, #2217), p-4EBP1 (Thr37/46, 1:1000, Cell Signaling, #2855), 4EBP1
154 (1:1000, Cell Signaling, #9644), nitrotyrosine (Santa Cruz, 1:1000, #32757) and ATF4 (1:1000, Thermo,
155 #PA5-27576). Following incubation, membranes were washed with TBS-tween and then probed for 1
156 hour at room temperature with anti-mouse or anti-rabbit secondary antibodies conjugated with either
157 horse radish peroxidase (Jackson ImmunoResearch, West Grove, PA, #115-035-003 and #115-035-144)
158 or infrared secondary (IRDye 680 and 800, LICOR, Lincoln, NE, #926-32210 and #926-68071). Images
159 were obtained by developing on a ChemiDoc XRS imaging system (BioRad, Hercules, CA) or Odyssey CLx
160 infrared imaging system (LICOR) and analyzed using ImageJ software (National Institutes of Health,
161 Bethesda, MD).

162 **Microarray Analysis**

163 Microarray analysis was performed on cDNA through the Affymetrix microarray analysis service
164 (ThermoFisher). Sham, Arrest, Sham+Met, and Arrest+Met mice were included in these studies with an
165 even distribution of males and females (total n=6 per group). Differential gene expression analysis was
166 performed using Transcription Analysis Console (Thermofisher). Gene-level p-values less than 0.05 were
167 considered significant for gene inclusion. Subsequent pathway analysis was performed to compare
168 untreated sham and arrest groups through Ingenuity Pathway Analysis (Qiagen). Complete datasets
169 were deposited in GEO (accession no. GSE176494).

170 **Cell Model**

171 AC16 cells, which are hybrid cell model derived from the fusion of adult ventricular myocytes with
172 stable, proliferating SV40 fibroblasts (29), were cultured in DMEM with 10% FBS and
173 penicillin/streptomycin (Thermo, #15140122). Cells were incubated overnight at 37° C in DMEM with
174 and without AICAR (1.25 mM) prior to hypoxia/reoxygenation (H/R) challenge. Immediately prior to
175 challenge, media was replaced with either DMEM (normoxia group) or Esumi buffer containing 137 mM
176 NaCl, 12 mM KCl, 0.5 mM $MgCl_2$, 0.9 mM $CaCl_2$, 20 mM HEPES, and 20 mM 2-deoxy-d-glucose at pH 6.2
177 (H/R group). Cells were challenged with either normoxia (20% oxygen, 5% CO_2) or hypoxia (1% oxygen,
178 5% CO_2) for 4 hours, then media was exchanged with normoxic DMEM. After 30 min of normoxia, cells
179 were stained with NucBlue Live (Hoechst 33342, Invitrogen) and NucGreen Dead (Sytox green,
180 Invitrogen) according to manufacturer recommendations and visualized on a Cell Insight CX7 HCX
181 Platform (Thermo) at 20x to quantify the ratio of living to dead cells. These cells were pelleted and flash
182 frozen for protein quantification.

183 **Protein Synthesis Assay**

184 The normoxia vs H/R challenge was repeated for protein synthesis assays using the methionine analog 1-
185 azidohomoalanine (AHA; Thermo). Immediately after normoxia/hypoxia, cell media was exchanged with
186 methionine free media (RPMI, Thermo) containing AHA for 30 min. After treatment, media was
187 removed, and cells fixed and permeabilized. The AHA reaction cocktail was added to cells to detect AHA
188 signaling as a marker of protein synthesis and cells were co-labeled with Hoecsht stain. Cells were
189 visualized for fluorescent signal and total fluorescent intensity quantified in a ring around the nuclei
190 using the Cell Insight CX7 HCX Platform.

191 **Respirometry and Hydrogen Peroxide Assay**

192 Oroboros high-resolution respirometry was performed on fresh whole-tissue homogenate using an
193 Oroboros Oxygraph-2K (Innsbruck, Austria). Homogenization was performed by adding 50 mg of frozen
194 LV to Mir05 buffer ($MgCl_2$-$6H_2O$ 3 mM, K^+MES 105 mM, taurine 20 mM, KH_2PO_4 10 mM, Hepes 20 mM,
195 d-sucrose 110 mM, and fatty acid-free BSA 1 g/l). After baseline respiration was established, 5 mM
196 pyruvate, 2 mM malate, and 10 mM glutamate (PMG) were added to assess respiratory capacity
197 through complex I, followed by ADP (2 mM) titrations to stimulate respiration. Next, 10 µM cytochrome
198 C was added to assess mitochondrial integrity, followed by 10 mM succinate to assess the combined
199 activity of Complex I + II, then 0.5 µM carbonyl cyanide 3-chlorophenylhydrazone (CCCP) to uncouple
200 the mitochondrial membrane and induce maximal respiration. Hydrogen peroxide levels were assessed
201 from these tissues using Amplex Red Assay (Thermo, #A22188) according to manufacturer instructions.

202 **Statistical Analysis**

203 Data were expressed as mean ± standard error in all figures. $P \leq 0.05$ was considered significant for all
204 comparisons. One-way ANOVA with Dunnett's multiple comparisons test was used to all compare
205 groups with the exception of Figure 8, in which student's t-test was used. All statistical analysis was
206 completed using Graphpad Prism 8 software (San Diego, CA).

207

208 **Results**

209 **Metformin pretreatment protects cardiac EF and is dependent on AMPK signaling**

210 To test the cardioprotective effects of metformin in CA, mice were pretreated for 2-weeks with
211 metformin prior to the CA procedure (Figure 1) and compared to untreated arrest mice. There were no
212 significant differences between groups to baseline animal characteristics, including the ratio of female
213 mice (Table 1), body weight (Table 1), or baseline EF (Figure 2A) in these mice. Twenty-four hours after
214 arrest, untreated arrest mice had significantly lower EF than untreated sham mice (Sham: 59.5±1.7%;
215 arrest: 41.1±2.7%, $p<0.0001$, Figure 2A), as expected based on our previous description of this model
216 (26). Metformin pretreatment significantly protected EF measured 24 hours after CA (Arrest+Met:
217 51.6±2.6%, $p<0.01$ vs. Arrest, Figure 2A). There were no changes to postoperative body temperature,
218 time to resuscitation, or time to extubation (Table 1). Sham mice pretreated with metformin had no
219 change to baseline characteristics or EF 24 hours after the procedure. These baseline and control
220 measures found no confounding variables.

221 Metformin has multiple potential modes of action (30), with AMPK activation being dominant in the
222 literature. Because of AMPK's role in cardiac resilience (25), we tested whether direct AMPK activation
223 was necessary and sufficient for the observed enhanced EF. Cohorts of mice were treated for 2-weeks
224 with the AMPK activator AICAR (31) or metformin and compound C, an established AMPK inhibitor (12).
225 Both groups underwent two weeks of intraperitoneal (IP) injections before CA and were evaluated by
226 echocardiography at baseline and twenty-four hours after arrest. No changes were observed in baseline
227 EF (Figure 2A) or baseline characteristics, including age, % female, or body weight compared to the
228 arrest group (Table 1). Like the metformin results, AICAR pretreated arrest mice had significantly
229 improved EF compared to untreated arrest mice at 24 hours post-CA, (Arrest+AICAR: 52.0±2.4%, $p<0.05$
230 vs. arrest, Figure 2A). Compound C not only prevented the beneficial effects of metformin on cardiac EF,
231 but also caused significantly reduced EF (Arrest+Met+Comp C: 30.0±2.9%) when compared to the
232 untreated arrest group ($p<0.05$). The AICAR pretreatment phenocopies metformin pretreatment, and
233 compound C blocks the benefit of metformin, suggesting that AMPK activation is necessary and
234 sufficient for the metformin-mediated protection of cardiac function after CA.

235 To determine AMPK activation status, we assessed phosphorylation of threonine-172 of the AMPKα
236 subunit in the myocardium (32). 24 hours after CA procedure, LVs from sham and arrest groups
237 (n=6/group) were assessed for p-AMPK, total AMPK, and glyceraldehyde 3-phosphate dehydrogenase
238 (GAPDH) protein expression and were normalized to the arrest group (Figure 2B, Supplemental Figure
239 1). p-AMPK/AMPK was not significantly changed between Sham (1.44±0.47), Arrest (1.00±0.17), and
240 Sham+Met (1.15±0.16) groups. p-AMPK/AMPK was elevated in the Arrest+Met mice (2.19±0.19, $p<0.01$
241 vs. Arrest) and Arrest+AICAR mice (1.91±0.31, $p<0.05$ vs. arrest), but unchanged in the
242 Arrest+Met+Comp C mice (1.024±0.12). Total AMPK was unchanged between the treatment groups
243 (Supplemental Figure 1). The strongest activation of AMPK was with metformin or AICAR plus arrest,
244 suggesting a synergistic effect of drug and arrest on activation at this time point.

245 **Metformin pretreatment protects against kidney injury and is dependent on AMPK signaling**

246 The effects of whole-body ischemia/reperfusion injury can be detected in peripheral tissues, particularly
247 in the kidney (26). Untreated arrest mice have significant kidney damage by tubular injury scoring
248 compared to untreated sham mice at one-day post-CA (sham: 0.11±0.04; arrest: 3.33±0.24, $p<0.0001$,

249 Figure 2C). Metformin pretreated sham mice have no evidence of damage by tubular injury scores
250 (0.14±0.04, p<0.0001 vs arrest). Metformin pretreated arrest mice had significantly lower tubular injury
251 scores (2.26±0.24, p<0.05) than the arrest group. AICAR pretreated arrest mice had lower injury scores
252 (1.45±0.42, p<0.001) than arrest mice, while Metformin + compound C mice had no protection evident
253 by score (2.54±0.47). To test peripheral markers as a proxy to tubular injury scores, serum markers of
254 kidney damage, creatinine and BUN, were also assessed in each group (Supplemental Figure 2). Serum
255 creatinine was significantly elevated in the arrest mice compared to sham (sham: 0.36±0.04 mg/dL;
256 arrest: 1.49±0.14 mg/dL, p<0.0001). There was no significant change to metformin pretreated arrest
257 mice (0.97±0.21 mg/dL), though significant changes were found in the AICAR arrest (0.67±0.25, p<0.01)
258 and Metformin + compound C mice (0.85±0.07, p<0.05) compared to sham. BUN was elevated in arrest
259 mice compared to sham (sham: 26.6±5.2 mg/dL; arrest: 153.9±28.4 mg/dL, p<0.001) but was unchanged
260 between arrest mice and Metformin pretreated arrest (121.2±28.0 mg/dL), AICAR arrest (85.7±8.9), and
261 Metformin + compound C mice (135.8±18.6). No changes were found when comparing the time to
262 kidney reperfusion between the untreated arrest and arrest treatment groups by Doppler flow analysis
263 of the renal artery (Table 1). Taken together, systemic activation of AMPK reduces histological markers
264 of kidney damage induced by CA, but 24-hour serum markers show limited sensitivity to this protection.

265 **Metformin causes broad transcriptome changes in sham and arrest mice**

266 To better understand the signaling changes caused by metformin therapy, transcriptomic analysis was
267 performed on LVs from Sham, Arrest, Sham+Met, and Arrest+Met groups (n=6/group) by microarray.
268 Differentially expressed genes were identified for three separate comparisons: Arrest vs. Sham,
269 Sham+Met vs. Sham, and Arrest+Met vs. Arrest (p<0.05, no fold restriction, Supplemental Figure 3).
270 Pathway analysis was then performed on these transcriptome changes through Ingenuity Pathway
271 Analysis. The top 15 most significantly changed pathways are included in Figure 3, along with z-score to
272 predict upregulation or downregulation of each pathway. Prominent pathways include changes to
273 autophagy, AMPK signaling, unfolded protein response, nuclear factor-erythroid 2-related factor 2
274 (NRF2) mediated oxidative stress, and eukaryotic initiation factor 2 (EIF2) signaling. We performed initial
275 confirmation studies for these pathways and focused on changes detectable at 24 hours. When no
276 supporting data were found, we advanced other pathway studies. When support was identified,
277 additional studies were done for confirmation.

278 **Metformin affects mitochondrial morphology and markers of autophagy**

279 Interestingly, autophagy pathway shows the most significant changes between Arrest and Sham and
280 Sham+Met and Sham, but not between Arrest+Met and Arrest. Because metformin has been reported
281 to increase cardiac mitophagy in cardiomyopathy (33,34) and autophagy was the top hit in two of the
282 sample comparisons, we evaluated protein expression for markers associated with autophagosome
283 formation, including p62/Sequestosome 1, a cargo receptor associated with degradation of
284 ubiquitinated proteins (35), and microtubule-associated protein light chain 3 (LC3) processing (Figure 4).
285 p62 expression (normalized to GAPDH) was not significantly changed between groups. The relative
286 levels of microtubule-associated protein light chain 3 (LC3), specifically levels of uncleaved (LC3-I) and
287 cleaved (LC3-II) forms, were also monitored as an indicator of changes in autophagy initiation (36).
288 Interestingly, the LC3-II to LC3-I ratio was significantly increased in untreated arrest mice (1.91±0.15)
289 compared to sham (1.00±0.18, p<0.01), whereas the metformin-pretreated arrest mice had significantly
290 reduced LC3-II/LC3-I (1.17±0.17) when compared to untreated arrest mice (p<0.05). LC3-I and LC3-II

291 expression levels (normalized to GAPDH) were not significantly changed between groups (data not
292 shown). The normalization of LC3-II/LC3-I may be interpreted as metformin restoration of mitophagy;
293 however, ischemia/reperfusion is well known to induce mitochondrial damage and mitophagy (37) and
294 reduction in mitochondrial damage could yield a similar change in LC3 ratios.

295 To begin to assess mitochondrial damage, we used electron microscopy to examine
296 mitochondrial structural changes among hearts from untreated sham, untreated arrest, and metformin-
297 pretreated arrest mice (Figure 5A). The untreated arrest mice showed a decrease in mitochondrial
298 perimeter and area (perimeter: 3.06±0.06 μm; area: 0.60±0.02 μm^2) when compared to sham
299 (perimeter: 3.81±0.09 μm; area: 0.87±0.04 μm^2, $p<0.0001$ for both measures) in cardiomyocytes (Figure
300 5B). Myocardium from metformin-pretreated arrest mice showed a modest but significant increase of
301 mitochondrial perimeter and area (perimeter: 3.33±0.07 μm; area: 0.70±0.03 μm^2) when compared to
302 that of untreated arrest mice ($p<0.05$ for both measures). Both the untreated arrest mice (0.76±0.001
303 μm, $p<0.0001$) and metformin-pretreated arrest mouse heart (0.75±0.01 μm; $p<0.0001$) had more
304 circular mitochondria than the untreated sham mouse (0.69±0.01 μm). These data demonstrate modest
305 changes in mitochondrial morphology at 24 hours post-CA, with normalization of mitochondrial area and
306 perimeter but not circularity in metformin-pretreated arrest mice compared to untreated arrest mice,
307 which may be consistent with diminished mitochondrial damage or normalization of membrane
308 dynamics.

309 Because of the change in mitochondrial architecture, we also looked at markers of
310 mitochondrial biogenesis and damage in the LVs to explain the protection by metformin. First,
311 representative proteins of mitochondrial respiratory complexes were assessed from LV extracts taken 24
312 hours after arrest from untreated sham, untreated arrest, metformin-pretreated sham, and metformin-
313 pretreated arrest mice (Figure 5C). There was a mild but statically significant elevation in a subunit of
314 complex II in the metformin-pretreated arrest mice (1.29±0.10) compared to untreated sham mice
315 (0.98±0.04, $p<0.01$); but otherwise, relative expression of representative proteins was unchanged across
316 the groups. Consistent with these results, we found no significant differences in Oroboros measurement
317 of mitochondrial oxygen consumption in heart homogenates in sham and arrest cohorts (Supplemental
318 Figure 4A). After sequential stimulation with PMG, ADP, Cytochrome C, succinate, and FCCP, we found
319 no significant differences in oxygen consumption rates (OCR). Prior work shows that mitochondrial
320 dysfunction induced by ischemia-reperfusion injury resolved in less than 24 hours (38,39), so this result
321 really only informs that the respiratory defect is not protracted in metformin+arrest heart.

322 **Metformin pretreatment protects against mtDNA damage after arrest**

323 We next examined mtDNA relative abundance and damage in the cardiac tissue from these
324 groups (Figure 5D). Unlike in failed hearts (40), the arrest group did not show a statistically significant
325 decrease in mtDNA levels at 24 hours post-CA, consistent with evidence above that mitochondria are
326 not being dramatically removed by autophagy. The metformin-pretreated arrest mice had slightly higher
327 relative mitochondrial DNA (mtDNA) levels (1.16±0.06) than untreated arrest mice (0.89±0.05, $p<0.05$),
328 but were not significantly different from the sham group (1.00±0.05). Importantly, the metformin-
329 pretreated arrest mice had significantly less mtDNA damage in a long extension assay (0.03±0.1
330 lesions/10kb mtDNA) than untreated arrest mice (0.59±0.16 lesions, $p<0.05$). There was no statistical
331 difference between sham and arrest+met groups. The small but significant increases in mtDNA and
332 complex II in the metformin-pretreated arrest mice could be consistent with an increase in

333 mitochondrial biogenesis, but the combined significant improvement in mitochondrial morphology and
334 mtDNA integrity suggests an improvement in overall mitochondrial quality, decreased damage, and are
335 in line with the changes in autophagy markers.

336 **Metformin pretreatment affects markers of mitochondrial dynamics**

337 To understand the alterations in mitochondrial morphology better, we examined the relative
338 levels of several proteins involved in establishing mitochondrial shape (Figure 5E). Mitofusin 2 (MFN2), a
339 mitochondrial outer membrane GTPase involved in fusion, had reduced expression in metformin-
340 pretreated arrest mice (Arrest+Met: 0.53±0.07) compared to all other groups (Sham: 1.00±0.10, $p<0.01$;
341 Arrest: 1.06±0.07, $p<0.001$; Sham+Met: 0.89±0.04, $p<0.05$). OPA1, also a dynamin-related GTPase that
342 resides in the inner membrane to perform fusogenic functions (41), followed a similar overall trend with
343 significantly reduced levels in metformin-pretreated arrest mice (0.75±0.04) when compared to
344 untreated arrest mice (1.13±0.10, $p<0.05$). In contrast, dynamin-related protein 1 (DRP1), whose activity
345 is regulated by its phosphorylation at Ser-616 (42), showed no significant change in p-DRP1/DRP1
346 between sham and arrest groups. Metformin pretreatment appeared to improve p-DRP1/DRP1 post-
347 arrest modestly, but the effect was not statistically significant, likely because the decline in p-DRP in
348 untreated arrest hearts was not significant. Indeed, while mitochondrial perimeter and area are
349 increasing with metformin-pretreatment in 24-hour post-arrest hearts, markers of fusion and fission are
350 not significantly changed by arrest (relative to sham), suggesting that these markers are not the driver of
351 those morphological changes. In fact, the MFN2 and OPA1 decrease and p-DRP1/DRP1 increase by
352 metformin pretreatment in arrested mice (relative to arrest mice) are moving in the opposite direction
353 from what would be expected to correct mitochondrial morphology. We suggest that other
354 mitochondrial quality control processes contribute to mitochondrial morphological rescue.

355 **Metformin pretreatment protects against changes to markers of protein synthesis**

356 Interestingly, the MFN2 decrease is consistent with the activation of autophagy (43,44), where it
357 is ubiquitinated and targeted for proteolysis. Metformin has been reported to impact heart autophagy
358 through AMPK signaling (33,34). To test engagement of autophagy in the CA model, LVs collected 24
359 hours after arrest from untreated sham, untreated arrest, metformin-pretreated sham, and metformin-
360 pretreated arrest mice were evaluated for markers of autophagy by Western blot analysis (Figure 6).
361 First, we evaluated mTOR activation as a crucial negative regulator of autophagy (45). As a positive
362 downstream marker of mTOR activity, S6 ribosomal protein (S6) phosphorylation at Ser-240/244 (p-S6)
363 was assessed (Figure 6A). Both the p-S6/GAPDH and p-S6/S6 showed that the mTOR pathway activity
364 was highest in the arrest + metformin. We suggest that mTOR is potentially highly activated in
365 arrest+metformin hearts at 24-hours post arrest. Because mTOR activity inhibits autophagy, the concept
366 that AMPK activation and subsequent mTOR inhibition to increase autophagy is insufficient to explain
367 the survival benefit of metformin.

368 EIF2 signaling was the most significantly altered pathway between the Arrest+Met and Arrest
369 groups (Figure 3) and is activated by mTOR (46,47). EIF2 signaling is commonly referred to as a marker of
370 the endoplasmic stress downstream of protein kinase RNA-like ER kinase (PERK) activation (48). In that
371 role, EIF2 activation promotes expression of activating transcription factors (ATFs) including ATF4, an
372 integrated stress response regulator, which is known to be activated by metformin (49,50). However, we
373 did not find any significant changes in ATF4 expression between our treatment groups (Supplemental

374 Figure 5). The mRNA changes driving EIF2 signaling are overwhelmingly related to ribosomal proteins
375 (Supplemental Figure 5B), leading us to explore markers of protein synthesis.

376 As both the EIF2 pathway and p-S6 activation increase mRNA translation, we next performed
377 additional Western blot analysis of eukaryotic translation initiation factor 4E-binding protein 1 (4EBP1).
378 4EBP1 is a repressor of mRNA translation (51), and when phosphorylated at Thr37/36, 4EBP1 releases
379 eukaryotic translation initiation factor 4E (eIF4E) and is degraded (Figure 6C). eIF4E. proceeds to
380 increase protein synthesis. We found that the ratio of p-4EBP1/4EBP1 was decreased in arrest mice
381 (0.76±0.05) when compared to sham (1.00±0.05, p<0.01; Figure 6B). The Sham+Met (0.89±0.05) group
382 was unchanged from Arrest; however, the Arrest+Met group (0.94±0.03) was significantly higher than
383 Arrest (p<0.05). Sham mice had higher p-4EB1/GAPDH (1.00±0.13) than Arrest mice (0.54±0.05, p<0.01),
384 while there was no change between the Arrest mice and the Sham+Met (0.56±0.04) or the Arrest+Met
385 (0.69±0.05) groups. Similarly, Sham mice had higher 4EBP1/GAPDH (1.00±0.09) vs. Arrest (0.71±0.03,
386 p<0.01), but there was no change between Arrest mice and Sham+Met (0.64±0.02) or Arrest+Met
387 (0.74±0). The elevation of p-S5, p-4EBP1 and activation of the EIF2 pathway strongly implicate activation
388 of mTOR in the promotion of translation that persists at 24-hours post-arrest.

389 **AICAR pretreatment protects against H/R changes to protein synthesis in a cell model**

390 To quantify protein synthesis changes, we replicated the hypoxic insult of CA in cell culture by
391 using AC16 cells (Figure 7A). Cells were pretreated overnight with AICAR, to mimic AMPK activation
392 specifically. Cells underwent normoxia or hypoxia (1% oxygen in Esumi buffer) for 4 hours prior to
393 reoxygenation with and without AICAR pretreatment. While p-AMPK/AMPK was unchanged between
394 groups (n=6, Figure 7B), we found that p-AMPK/GAPDH was elevated in untreated H/R cells (1.60±0.21)
395 compared to untreated normoxia (1.00±0.10, p<0.001) and AICAR normoxia cells (1.39±0.25, p<0.01).
396 There was no change between untreated H/R and H/R+AICAR cells (1.89±0.20). AMPK/GAPDH was also
397 elevated in untreated H/R cells (2.18±0.21) vs untreated normoxia (1.00±0.15, p<0.05), but unchanged
398 compared to AICAR normoxia (1.37±0.37) and AICAR H/R cells (1.58±0.24).

399 p-S6/S6 was decreased in the untreated H/R cells (0.78±0.01) compared to untreated normoxia
400 (1.00±0.06, p<0.01), and unchanged compared to AICAR normoxia (0.91±0.02) but was significantly
401 higher in the AICAR H/R cells (0.93±0.05, p<0.05). Similar changes were found in the p-S6/GAPDH and
402 S6/GAPDH comparisons. Finally, p-4EBP1/4EBP1 was decreased in untreated H/R cells (0.72±0.01)
403 compared to untreated normoxia (1.00±0.08, p<0.05), and unchanged compared to AICAR normoxia
404 (0.83±0.03) and AICAR H/R cells (0.87±0.06). However, p-4EBP1 was significantly lower in the untreated
405 H/R cells (0.56±0.01) compared to all other groups (untreated normoxia: 1.00±0.04, p<0.001, AICAR
406 normoxia; 0.74±0.04, p<0.01, AICAR H/R: 0.74±0.04, p<0.01). There was no change to percent of dead
407 cells after reoxygenation in any of the cell groups (Figure 7C).

408 Protein synthesis was quantified for each cell groups by measuring fluorescent intensity of
409 labeled AHA given immediately after reoxygenation (n=3000-5000 cells/group). The fluorescent intensity
410 was lower in the untreated H/R cells (1397713±12864) compared to untreated normoxia
411 (2021451±13931, p<0.0001) and AICAR normoxia cells (1969457±16463, p<0.0001; Figure 7D). The
412 AICAR H/R cells had significantly higher intensity (1651628±16842) compared to the untreated H/R cells
413 (p<0.0001). These *in vitro* data suggestion that activation of AMPK would restore protein translation
414 disrupted by ischemia/reperfusion injury in heart.

415 **Metformin does not improve outcomes as a rescue therapy**

416 To test metformin's efficacy as rescue therapy in our model, metformin was given directly into the LV in
417 a cohort of mice (n=7) at the time of resuscitation (1,250 µg/kg). When compared to the arrest mice
418 described in Figure 2, there was no change to EF one day after CA (arrest rescue metformin: 42.9±2.4%,
419 Figure 8A). Similarly, there was no change in tubular injury score (2.54±0.423, Figure 8A), creatinine
420 (1.2±0.25, Supplemental Figure 6), or BUN (155.3±14.2) when compared to untreated arrest mice.
421 Baseline EF (61.1±2.1) was not significantly different from the arrest mice. These data are consistent
422 with the notion that metabolic adaptation is required for metformin protection after CA.

423 Hearts from these mice were collected and Western blots performed comparing untreated
424 arrest vs arrest with rescue metformin. There was no change to p-AMPK/AMPK, p-AMPK/GAPDH, or
425 AMPK/GAPDH between treatment groups (Figure 8B&C). p-S6/S6 and S6/GAPDH were unchanged
426 between groups, though there was a reduction in p-S6/GAPDH in the arrest + rescue metformin cohort
427 (0.75±0.08) when compared to untreated arrest mice (1.00±0.03, $p<0.05$). There was a mild reduction in
428 p-4EBP1/4EBP1 in the arrest + rescue metformin mice (0.88±0.04) when compared to untreated arrest
429 mice (1.00±0.02, $p<0.05$), but p-4EBP1/GAPDH and 4EBP1/GAPDH were unchanged. These differences in
430 magnitude and duration of activation of these pathways in this model may account for the failure as a
431 rescue therapy.

432

433 **Discussion**

434 Our group recently performed a retrospective analysis of diabetic CA patients with and without
435 metformin therapy before arrest and found that metformin improved markers of cardiac and renal
436 damage acutely after CA (9). This exciting result prompted the search for reports of preclinical models to
437 identify the molecular pathways involved. Of particular relevance are studies of a 9-min rat asphyxial
438 model. Metformin pretreatment has neurologic and 7-day survival benefits but focuses on neuronal
439 markers without measures of cardiac and renal outcomes (21). More recently, a 10-min asphyxial rat
440 model with post-CA treatment demonstrated improved 3-day survival and neurological function,
441 involving normalization of brain activity without activation of AMPK, but also did not examine cardiac
442 and renal function. Our current data suggest that metformin-mediated cardiac protection may also
443 promote survival. Indeed, the lack of AMPK activation in the 2-hours post-treatment brain could be
444 consistent with protection arising from other metformin activities. Unfortunately, acute metformin
445 rescue was unsuccessful in our myocardial stunning model, so potential confounders in interpretation
446 among these studies remain.

447 Metformin pretreatment has previously been shown to decrease scar size in reversible coronary
448 artery ligation (24,52–56) and *ex vivo* whole-heart ischemia-reperfusion (24,57). However, studies of
449 metformin's effects on cardiac function have primarily utilized ischemia-reperfusion injury models with
450 ischemic periods of 25-30 minutes. The long ischemic duration in these models involves substantial
451 cardiomyocyte necrosis. Much of metformin's beneficial effect has been attributed to reducing mPTP-
452 mediated cell death (58). In contrast, our data demonstrate metformin's protection of *in vivo* EF in a CA
453 model (Figure 1) that features an 8-minute ischemia period without evidence of cardiac cell death (26).
454 We, therefore, set out to identify intracellular processes that adapt the cardiomyocyte to maintain
455 function rather than alter cell survival.

456 Metformin pretreatment has pleiotropic effects involving many molecular pathways, including
457 reducing oxidative stress, inhibiting apoptosis, inhibiting complex I, and activating AMPK signaling
458 (20,24,59,60). In our CA mouse model, we find that AMPK activation is necessary and sufficient to enact
459 metformin's cardioprotective effects. Mice pretreated with AICAR, an AMP-mimetic known to activate
460 AMPK (50), had preserved EF one day after CA compared to the untreated arrest mice (Figure 2A).
461 Conversely, mice pretreated with metformin with the AMPK inhibitor compound C showed no
462 improvement in EF one day after arrest compared to the untreated arrest mice. AICAR conferred similar
463 renal protection as measured by tubular injury score, and the protective effects of metformin on the
464 kidney were negated by compound C (Figure 2C). Interestingly, we did not find evidence of p-
465 AMPK/AMPK changes between the arrest and sham groups by Western blot (Figure 2B), despite
466 indicated AMPK changes in transcriptome pathway analysis (Figure 3). This phosphorylation status of
467 AMPK may have recovered at the time point evaluated (24 hours after arrest), while the continued
468 effects of metformin and AICAR are observed.

469 Pathway analysis was performed on microarray data collected from LVs of Sham, Arrest,
470 Sham+Met, and Arrest+Met mice. A comparison of arrest to sham mice (Figure 3) implicates autophagy
471 and AMPK signaling in our model. Given the evidence of metformin's AMPK-dependent effects (Figure
472 2), it should be expected that metformin therapy causes similar pathway changes in the sham mouse or
473 the untreated arrest model. Several signaling changes were observed when comparing untreated arrest
474 to untreated sham mice (Figure 3, top) when comparing the metformin-treated sham to untreated sham

475 mice (Figure 3, middle). These shared pathways include activation of autophagy, NRF-2 mediated
476 oxidative stress response, NAD signaling, and xenobiotic metabolism signaling. Given this overlap, it is
477 unsurprising that signaling pathways are less profound when comparing the metformin pretreated
478 arrest and untreated arrest mice (Figure 3, bottom). Interestingly, the strongest hit in the Arrest+Met
479 mice compared to the arrest animals was EIF2 signaling, which may suggest an increased ability to
480 support the initiation of translation for protein synthesis after CA.

481 We focused on transcriptional pathways that were altered at the time of cardiac assessment,
482 which showed overt cardiac dysfunction (Figure 1A). Autophagy, AMPK signaling, unfolded protein
483 response, Nrf2-mediated oxidative stress, and EIF2 signaling show differences in transcriptional
484 signatures between Sham, Arrest and Arrest+Met at 24 hours post-arrest. The absence of changes in
485 gene expression sham arrest and metformin arrest, i.e., metformin may be blocking the alterations in
486 the arrest conditions. In the process, we observed whether given pathway markers being tested showed
487 activation or normalization, i.e., regression to sham levels. For autophagy, the pathway was activated in
488 Arrest vs. Sham and Sham+Met vs. Sham but *not* in Arrest+Met vs.Arrest, suggesting that the pathway
489 wasn't accelerated at the time of analysis. Normalization of mitochondrial function, mitochondrial
490 morphology, LC3-II/I ratios, and hyperphosphorylation of S6, which is inhibitory for autophagy (61), are
491 consistent with the non-activation of autophagy. Although mtDNA lesions are decreased, which could be
492 compatible with accelerated autophagy, the increase in total mtDNA levels and mitochondrial Complex
493 II may indicate some compensatory mitochondrial biogenesis. The significant decreases (i.e., not
494 normalization) of OPA1 and MFN2 and increase in p-DRP1 levels in Arrest+Met relative to Arrest alone
495 (Figure 5E) would suggest a change in mitochondrial dynamics, but measure mitochondrial area and
496 perimeter are increasing mitochondrial size (Figure 5B) instead of the expected shift to a more
497 fragmented shape due to changes in those proteins (41,62,63). We did not detect oxidative protein
498 modification (Supplemental Figure 4), which is known to be primarily mitochondrial proteins damaged
499 at early timepoints (38,39), suggesting that oxidant activating the Nrf2 signaling pathway may have been
500 resolved by 24 hours post-CA. This is in line with the normalization of mitochondrial function by 24
501 hours post reperfusion described by others and the lack of differences in respiration described herein
502 (Supplemental Figure 4A).

503 The hyperactivation of p-S6 also showed an accelerated response at 24 hours post-CA in
504 Arrest+Met compared to Arrest alone samples. Initial tests of ATF4 activation downstream of S6K
505 activation did not support the unfolded protein response's involvement at this time. We speculated that
506 p-S6 was not only indicating that AMPK stimulated activity inhibited mTOR, which activated p70S6K, but
507 also the downstream activation of translation (Figure 6C). We also show alterations to the
508 phosphorylation status of the translation repressor protein 4EBP1 in the untreated arrest mice, which is
509 normalized in the arrest mice pretreated with metformin (Figure 6B). Phosphorylated 4EBP1 is
510 dissociated from the translation initiation factor eIF4E (Figure 6C), allowing eIF4E to initiate translation
511 (64).

512 To confirm changes in protein synthesis, we performed H/R studies of AC16 cells. We found that
513 4 hours of ischemia in these cells was enough to insult to drive Western blot markers without causing
514 cell death (Figure 7A, C). Cell homogenates in the untreated H/R groups have elevated p-AMPK/GAPDH
515 compared to normoxia, and AICAR treated normoxia cells (Figure 7B). However, we did not find
516 superactivation of p-AMPK in the AICAR pretreated H/R cells. p-S6/S6 was significantly decreased in the
517 untreated H/R cells compared to normoxia but preserved in the AICAR pretreated H/R group. Similarly,

518 p-4EBP1/4EBP1 was reduced in the H/R mice compared to untreated normoxia cells but preserved in
519 the AICAR pretreated group. The protective effects of AICAR on p-S6/S6 and p-4EBP1/4EBP1 were
520 comparable to those seen by metformin in the animal model.

521 It should be noted that the p-S6/S6 is lower in the untreated H/R cells compared to the
522 untreated normoxia cells, which is discordant with changes seen in the metformin-treated mice;
523 however, the mouse model was complicated by epinephrine injection and surgical handling as well as
524 delayed tissue collection (24 hours in mice, compared to 30 min in cells), which may explain the
525 differences in p-S6/S6 results between the *in vivo* and *in vitro* systems. Importantly, we found that
526 untreated H/R cells reduced protein translation compared to untreated normoxia cells, partially
527 protected by AICAR pretreatment (Figure 7D). While these data suggest that AMPK activation can
528 preserve translation in ischemia/reperfusion stressed cardiomyocytes, additional studies will be needed
529 to establish to what extent such preservation contributes to cardiomyocyte resilience *in vivo*.

530 Finally, we performed a direct injection of metformin into the LV at the time of resuscitation to
531 test the effects of metformin as rescue therapy. To minimize animal injury, we compared the rescue
532 metformin cohort to the large arrest cohort described in Figure 2. However, we completed the analysis
533 of EF and kidney changes in a blinded fashion. This small cohort of mice had no evidence of improved EF
534 or kidney injury compared to the arrest group (Figure 8, Supplemental Figure 7). There has been some
535 controversy concerning the use of metformin after cardiac insult. While several preclinical studies have
536 found beneficial effects of metformin therapy when given at the reperfusion (24,56,59,65), this
537 protection was not evident in a pig model of myocardial infarction (66). Our data suggest that while
538 metformin as a pretreatment protects both the heart and the kidneys against ischemia-reperfusion
539 injury, this protection depends on adaptive mechanisms before the insult and the nature of the insult.
540 When used as rescue therapy, metformin did increase p-S6/S6 as seen in the metformin pretreatment
541 group, but p-4EBP1/4EBP1 was significantly lower in the rescue metformin mice. This supports the
542 notion that metformin's support for mRNA translation after CA requires preconditioning, rather than
543 rescue therapy.

544 There are limitations to the results observed in this study. First, while metformin provided clear
545 evidence of renal protection as measured by tubular injury (Figure 2C), these results are less clear when
546 comparing serum markers of kidney injury, including creatinine and BUN. Further, we found unexpected
547 protection against renal damage in the Arrest+Met+Comp C cohort when compared to Arrest, which
548 may suggest an additional signaling component in the kidney or varying degrees of AMPK activation
549 between the heart and the kidney. However, these serum measurements depend on additional
550 physiologic factors, such as animal fluid status or peripheral tissue breakdown, which may complicate
551 their interpretation. For this reason, we consider tubular injury score a superior marker of damage (67).
552 This renal damage does not appear to depend on kidney reperfusion time (Table 1). However, this
553 reperfusion time was measured by doppler tracing of the renal artery, which may not have the
554 sensitivity to fully detect ischemic duration without contrast imaging (68). Regarding the rescue therapy,
555 the use of intravenous metformin was calculated based on pharmacologic rodent studies comparing oral
556 to intravenous metformin bioavailability (69). The concentration used was 10-times larger than an
557 intravenous dose of metformin used as rescue therapy in a mouse infarction model (56), so it is unlikely
558 that this concentration did not exert a significant effect.

559 In summary, we demonstrate that pretreatment with metformin protects against myocardial
560 stunning and renal injury in a mouse model of CA. Our CA mouse involves cardiac injury without cardiac
561 cell death, making it a more focused system to study metformin's mechanism of action. Direct AMPK
562 activation and inhibition studies confirmed that AMPK activation is necessary and sufficient for the
563 cardiac and renal benefits observed with metformin treatment. While multiple molecular mechanisms
564 exist downstream of AMPK activation that may affect these outcomes, microarray data and Western
565 blot changes suggest that preservation of mRNA translation may be a major mechanism underlying
566 metformin's effects. Preserved mRNA translation and protein synthesis were also found in a cell model
567 of H/R when pretreated with AICAR. Unfortunately, these findings did not translate into use as rescue
568 therapy, suggesting that metformin's effects require a degree of adaptation to confer tissue protection.

569

Acknowledgments

CR and BK were responsible for the conceptualization of these studies. CR designed the methodology, and with CL, KR, and EG performed the investigation. Formal analyses were performed by CR, CL, TC, EG, and SSL. TC and DS completed visualization. CR, SSL, and BK wrote the manuscript. SSL and BK supervised the project, and BK provided resources for its completion. All authors reviewed the final manuscript and are responsible for its integrity.

Sources of Funding

Research reported in this manuscript was supported by: American Heart Association Transformational Project Award 18TPA34230048 (to BK), NIH Instrument Grant for Advanced High-Resolution Rodent Ultrasound Imaging System 1S10OD023684-01A1, NIH Training Program in Imaging Sciences in Translational Cardiovascular Research 5T32HL129964-02, NIH F32HL156428 (to CR), and Richard K. Mellon Institute Award for postdoctoral trainees (to TC).

Disclosures

None of the authors have financial disclosures or conflicts of interest

587 **References**

588 1. Aparicio HJ, Benjamin EJ, Callaway CW, et al. *Heart Disease and Stroke Statistics-2021 Update A*
589 *Report from the American Heart Association*.; 2021. doi:10.1161/CIR.0000000000000950

590 2. Zipes D, Wellens HJJ. Sudden Cardiac Death. *Circulation*. 1998;98(21):2334-2351.

591 3. Mongardon N, Dumas F, Ricome S, et al. Postcardiac arrest syndrome: from immediate
592 resuscitation to long-term outcome. *Ann Intensive Care*. 2011;1(45):1-11.

593 4. Neumar RW, Nolan JP, Adrie C, et al. Post-cardiac arrest syndrome: Epidemiology,
594 pathophysiology, treatment, and prognostication a consensus statement from the International
595 Liaison Committee on Resuscitation. *Circulation*. 2008;118(23):2452-2483.
596 doi:10.1161/CIRCULATIONAHA.108.190652

597 5. Ruiz-Bailén M, Aguayo De Hoyos E, Ruiz-Navarro S, et al. Reversible myocardial dysfunction after
598 cardiopulmonary resuscitation. *Resuscitation*. 2005;66(2):175-181.
599 doi:10.1016/j.resuscitation.2005.01.012

600 6. Chang WT, Ma MHM, Chien KL, et al. Postresuscitation myocardial dysfunction: Correlated
601 factors and prognostic implications. *Intensive Care Med*. 2007;33(1):88-95. doi:10.1007/s00134-
602 006-0442-9

603 7. Park YS, Choi YH, Oh JH, et al. Recovery from acute kidney injury as a potent predictor of survival
604 and good neurological outcome at discharge after out-of-hospital cardiac arrest. *Crit Care*.
605 2019;23(1):1-11. doi:10.1186/s13054-019-2535-1

606 8. Storm C, Krannich A, Schachtner T, et al. Impact of acute kidney injury on neurological outcome
607 and long-term survival after cardiac arrest – A 10 year observational follow up. *J Crit Care*.
608 2018;47:254-259. doi:10.1016/j.jcrc.2018.07.023

609 9. Rutledge CA, Kaufman BA, Dezfulian C, Elmer J. Metformin Protects Against Cardiac and Renal
610 Damage in Diabetic Cardiac Arrest Patients. *Resuscitation*. 2022;174(January):42-46.
611 doi:10.1016/j.resuscitation.2022.03.017

612 10. Stumvoll M, Nurjhan N, Perriello G, Dailey G, Gerich JE. Metabolic Effects of Metformin in Non-
613 Insulin-Dependent Diabetes Mellitus. *N Engl J Med*. 1995;333(9):550-554.
614 doi:10.1056/nejm199508313330903

615 11. Wiernsperger NF, Bailey CJ. The Antihyperglycaemic Effect of Metformin. *Drugs*. 1999;58:31-39.
616 doi:10.2165/00003495-199958001-00009

617 12. Zhou G, Goodyear LJ, Moller DE, et al. Role of AMP-activated protein kinase in mechanism of
618 metformin action Find the latest version : Role of AMP-activated protein kinase in mechanism of
619 metformin action. *J Clin Invest*. 2001;108(8):1167-1174. doi:10.1172/JCI200113505.Introduction

620 13. Maruthur NM, Tseng E, Hutfless S, Wilson LM, Suarez-cuervo C. Diabetes Medications as
621 Monotherapy or Metformin-Based Combination Therapy for Type 2 Diabetes. *Ann Intern Med*.
622 2016;164:740-751. doi:10.7326/M15-2650

623 14. Han Y, Xie H, Liu Y, Gao P, Yang X, Shen Z. Effect of metformin on all cause and cardiovascular
624 mortality in patients with coronary artery diseases: a systematic review and an updated
625 meta analysis. *Cardiovasc Diabetol*. 2019;18(96):1-16. doi:10.1186/s12933-019-0900-7

626 15. Crowley MJ, Diamantidis CJ, Mcduffie JR, et al. Clinical Outcomes of Metformin Use in
627 Populations With Chronic Kidney Disease , Congestive Heart Failure, or Chronic Liver Disease. *Ann*
628 *Intern Med*. 2017;166:191-200. doi:10.7326/M16-1901

629 16. Bell S, Farran B, Mcgurnaghan S, et al. Risk of acute kidney injury and survival in patients treated
630 with Metformin: an observational cohort study. *BMC Nephrol*. 2017;18(163):1-8.
631 doi:10.1186/s12882-017-0579-5

632 17. Hassan FI, Sc M, Didari T, et al. A Review on The Protective Effects of Metformin in Sepsis-
633 Induced Organ Failure. 2020;21(4). doi:10.22074/cellj.2020.6286.Introduction

634 18. Jochmans S, Alphonsine JE, Chelly J, et al. Does metformin exposure before ICU stay have any
635 impact on patients' outcome? A retrospective cohort study of diabetic patients. *Ann Intensive*
636 *Care*. 2017;7(116):1-9. doi:10.1186/s13613-017-0336-8

637 19. Reitz K, Marroquin O, Zenati M, et al. Association Between Preoperative Metformin Exposure and
638 Postoperative Outcomes in Adults With Type 2 Diabetes. *JAMA Surg*. 2020;155(6).
639 doi:10.1001/jamasurg.2020.0416.Association

640 20. Cameron AR, Morrison VL, Levin D, et al. Anti-Inflammatory Effects of Metformin Irrespective of
641 Diabetes Status. *Circ Res*. 2016;119:652-665. doi:10.1161/CIRCRESAHA.116.308445

642 21. Zhu J, Liu K, Huang K, et al. Metformin improves neurologic outcome Via AMP-activated protein
643 kinase-mediated autophagy activation in a rat model of cardiac arrest and resuscitation. *J Am*
644 *Heart Assoc*. 2018;7(12). doi:10.1161/JAHA.117.008389

645 22. Shoaib M, Choudhary RC, Chillale RK, et al. Metformin-mediated mitochondrial protection post-
646 cardiac arrest improves EEG activity and confers neuroprotection and survival benefit. *FASEB J*.
647 2022;36(5):1-16. doi:10.1096/fj.202200121R

648 23. Chen Q, Lesnefsky EJ. Metformin and myocardial ischemia and reperfusion injury: Moving toward
649 "prime time" human use? *Transl Res*. 2020;229:1-4. doi:10.1016/j.trsl.2020.10.006

650 24. Higgins L, Palee S, Chattipakorn SC, Chattipakorn N. Effects of metformin on the heart with
651 ischaemia-reperfusion injury: Evidence of its benefits from in vitro, in vivo and clinical reports.
652 *Eur J Pharmacol*. 2019;858(April):172489. doi:10.1016/j.ejphar.2019.172489

653 25. Cao Y, Bojjireddy N, Kim M, et al. Activation of γ2-AMPK suppresses ribosome biogenesis and
654 protects against myocardial ischemia/reperfusion injury. *Circ Res*. 2017;121(10):1182-1191.
655 doi:10.1161/CIRCRESAHA.117.311159

656 26. Rutledge CA, Chiba T, Redding K, et al. A novel ultrasound-guided mouse model of sudden cardiac
657 arrest. *PLoS One*. 2020;15(12):1-14. doi:10.1371/journal.pone.0237292

658 27. Rutledge C, Cater G, McMahon B, et al. Commercial 4-dimensional echocardiography for murine
659 heart volumetric evaluation after myocardial infarction. *Cardiovasc Ultrasound*. 2020;18(1):1-10.
660 doi:10.1186/s12947-020-00191-5

661 28. Lang RM, Bierig M, Devereux RB, et al. Recommendations for chamber quantification: A report
662 from the American Society of Echocardiography's guidelines and standards committee and the
663 Chamber Quantification Writing Group, developed in conjunction with the European Association
664 of Echocardiograph. *J Am Soc Echocardiogr*. 2005;18(12):1440-1463.
665 doi:10.1016/j.echo.2005.10.005

666 29. Davidson MM, Nesti C, Palenzuela L, et al. Novel cell lines derived from adult human ventricular
667 cardiomyocytes. *J Mol Cell Cardiol*. 2005;39(1):133-147. doi:10.1016/j.yjmcc.2005.03.003

668 30. Xu X, Lu Z, Fassett J, et al. Metformin protects against systolic overload-induced heart failure
669 independent of AMP-activated protein kinase α2. *Hypertension*. 2014;63(4):723-728.
670 doi:10.1161/HYPERTENSIONAHA.113.02619

671 31. Corton JM, Gillespie JG, Hawley SA, Hardie DG. 5-Aminoimidazole-4-Carboxamide
672 Ribonucleoside: A Specific Method for Activating AMP-Activated Protein Kinase in Intact Cells?
673 *Eur J Biochem*. 1995;229(2):558-565. doi:10.1111/j.1432-1033.1995.tb20498.x

674 32. Stein SC, Woods A, Jones NA, Davison MD, Cabling D. The regulation of AMP-activated protein
675 kinase by phosphorylation. *Biochem J*. 2000;345(3):437-443. doi:10.1042/0264-6021:3450437

676 33. Kanamori H, Naruse G, Yoshida A, et al. Metformin Enhances Autophagy and Provides
677 Cardioprotection in δ-Sarcoglycan Deficiency-Induced Dilated Cardiomyopathy. *Circ Hear Fail*.
678 2019;12(4):1-13. doi:10.1161/CIRCHEARTFAILURE.118.005418

679 34. Xie Z, Lau K, Eby B, et al. Improvement of cardiac functions by chronic metformin treatment is
680 associated with enhanced cardiac autophagy in diabetic OVE26 mice. *Diabetes*. 2011;60(6):1770-
681 1778. doi:10.2337/db10-0351

682 35. Seibenhener ML, Babu JR, Geetha T, Wong HC, Krishna NR, Wooten MW. Sequestosome 1/p62 Is
683 a Polyubiquitin Chain Binding Protein Involved in Ubiquitin Proteasome Degradation. *Mol Cell*
684 *Biol*. 2004;24(18):8055-8068. doi:10.1128/mcb.24.18.8055-8068.2004

685 36. Li L, Xu J, He L, et al. The role of autophagy in cardiac hypertrophy. *Acta Biochim Biophys Sin*
686 *(Shanghai)*. 2016;48(6):491-500. doi:10.1093/abbs/gmw025

687 37. Yang M, Linn BS, Zhang Y, Ren J. Mitophagy and mitochondrial integrity in cardiac ischemia-
688 reperfusion injury. *Biochim Biophys Acta - Mol Basis Dis*. 2019;1865(9):2293-2302.
689 doi:10.1016/j.bbadis.2019.05.007

690 38. Bush L, Shlafer M, Haack D, Lucchesi B. Time-dependent changes in canine cardiac mitochondrial
691 function and ultrastructure resulting from coronary occlusion and reperfusion. *Basic Res Cardiol*.
692 1980;(75):555-571.

693 39. Dezfulian C, Shiva S, Alekseyenko A, et al. Nitrite therapy after cardiac arrest reduces reactive
694 oxygen species generation, improves cardiac and neurological function, and enhances survival via
695 reversible inhibition of mitochondrial complex I. *Circulation*. 2009;120(10):897-905.
696 doi:10.1161/CIRCULATIONAHA.109.853267

697 40. Karamanlidis G, Nascimben L, Couper GS, Shekar PS, Del Monte F, Tian R. Defective DNA
698 replication impairs mitochondrial biogenesis in human failing hearts. *Circ Res*. 2010;106(9):1541-
699 1548. doi:10.1161/CIRCRESAHA.109.212753

700 41. Ge Y, Shi X, Boopathy S, McDonald J, Smith AW, Chao LH. Two forms of Opa1 cooperate to
701 complete fusion of the mitochondrial inner-membrane. *Elife*. 2020;9:1-22. doi:10.1101/739078

702 42. Marsboom G, Toth PT, Ryan JJ, et al. Dynamin-related protein 1-mediated mitochondrial mitotic
703 fission permits hyperproliferation of vascular smooth muscle cells and offers a novel therapeutic
704 target in pulmonary hypertension. *Circ Res*. 2012;110(11):1484-1497.
705 doi:10.1161/CIRCRESAHA.111.263848

706 43. Xiong W, Ma Z, An D, et al. Mitofusin 2 participates in mitophagy and mitochondrial fusion
707 against angiotensin II-induced cardiomyocyte injury. *Front Physiol*. 2019;10(APR):1-12.
708 doi:10.3389/fphys.2019.00411

709 44. Benischke AS, Vasanth S, Miyai T, et al. Activation of mitophagy leads to decline in Mfn2 and loss
710 of mitochondrial mass in Fuchs endothelial corneal dystrophy. *Sci Rep*. 2017;7(1):1-11.
711 doi:10.1038/s41598-017-06523-2

712 45. Sciarretta S, Maejima Y, Zablocki D, Sadoshima J. The Role of Autophagy in the Heart. *Annu Rev*
713 *Physiol*. 2018;80:1-26. doi:10.1146/annurev-physiol-021317-121427

714 46. Cagnetta R, Wong HHW, Frese CK, Mallucci GR, Krijgsveld J, Holt CE. Noncanonical Modulation of
715 the eIF2 Pathway Controls an Increase in Local Translation during Neural Wiring. *Mol Cell*.
716 2019;73(3):474-489.e5. doi:10.1016/j.molcel.2018.11.013

717 47. Rios-Fuller TJ, Mahe M, Walters B, et al. Translation regulation by eif2α phosphorylation and
718 mtorc1 signaling pathways in non-communicable diseases (Ncds). *Int J Mol Sci*. 2020;21(15):1-26.
719 doi:10.3390/ijms21155301

720 48. Bertolotti A, Zhang Y, Hendershot LM, Harding HP, Ron D. Dynamic interaction of BiP and ER
721 stress transducers in the unfolded-protein response. *Nat Cell Biol*. 2000;2(6):326-332.
722 doi:10.1038/35014014

723 49. Quentin T, Steinmetz M, Poppe A, Thoms S. Metformin differentially activates ER stress signaling
724 pathways without inducing apoptosis. *DMM Dis Model Mech*. 2012;5(2):259-269.
725 doi:10.1242/dmm.008110

726 50. Harding HP, Zhang Y, Zeng H, et al. An integrated stress response regulates amino acid
727 metabolism and resistance to oxidative stress. *Mol Cell*. 2003;11(3):619-633. doi:10.1016/S1097-
728 2765(03)00105-9

729 51. Brunn GJ, Hudson CC, Sekulić A, et al. Phosphorylation of the translational repressor PHAS-I by
730 the mammalian target of rapamycin. *Science (80-)*. 1997;277(5322):99-101.
731 doi:10.1126/science.277.5322.99

732 52. Paiva MA, Gonçalves LM, Providência LA, Davidson SM, Yellon DM, Mocanu MM. Transitory
733 activation of AMPK at reperfusion protects the ischaemic-reperfused rat myocardium against
734 infarction. *Cardiovasc Drugs Ther*. 2010;24(1):25-32. doi:10.1007/s10557-010-6222-3

735 53. Solskov L, Løfgren B, Kristiansen SB, et al. Metformin induces cardioprotection against
736 ischaemia/reperfusion injury in the rat heart 24 hours after administration. *Basic Clin Pharmacol*
737 *Toxicol*. 2008;103(1):82-87. doi:10.1111/j.1742-7843.2008.00234.x

738 54. Whittington HJ, Hall AR, McLaughlin CP, Hausenloy DJ, Yellon DM, Mocanu MM. Chronic
739 metformin associated cardioprotection against infarction: Not just a glucose lowering
740 phenomenon. *Cardiovasc Drugs Ther*. 2013;27(1):5-16. doi:10.1007/s10557-012-6425-x

741 55. Gundewar S, Calvert, John W, Jha S, et al. Activation of AMPK by Metformin Improves Left
742 Ventricular Function and Survival in Heart Failure. *Circ Res*. 2009;454(1):42-54.
743 doi:10.1161/CIRCRESAHA.108.190918.Activation

744 56. Calvert JW, Gundewar S, Jha S, et al. Acute metformin therapy confers cardioprotection against
745 myocardial infarction via AMPK-eNOS- mediated signaling. *Diabetes*. 2008;57(3):696-705.

746 doi:10.2337/db07-1098

747 57. Bhamra GS, Hausenloy DJ, Davidson SM, et al. Metformin protects the ischemic heart by the Akt-
748 mediated inhibition of mitochondrial permeability transition pore opening. *Basic Res Cardiol*.
749 2008;103(3):274-284. doi:10.1007/s00395-007-0691-y

750 58. Emelyanova L, Bai X, Yan Y, et al. Biphasic effect of metformin on human cardiac energetics.
751 *Transl Res*. Published online 2020. doi:10.1016/j.trsl.2020.10.002

752 59. Mohsin AA, Chen Q, Quan N, et al. Mitochondrial complex I inhibition by metformin limits
753 reperfusion injury. *J Pharmacol Exp Ther*. 2019;369(2):282-290. doi:10.1124/jpet.118.254300

754 60. Lesnefsky EJ, Chen Q, Tandler B, Hoppel CL. Mitochondrial Dysfunction and Myocardial Ischemia-
755 Reperfusion: Implications for Novel Therapies. *Annu Rev Pharmacol Toxicol*. 2017;57:535-565.
756 doi:10.1146/annurev-pharmtox-010715-103335

757 61. Blommaart EFC, Luiken JJFP, Blommaart PJE, Van Woerkom GM, Meijer AJ. Phosphorylation of
758 ribosomal protein S6 is inhibitory for autophagy in isolated rat hepatocytes. *J Biol Chem*.
759 1995;270(5):2320-2326. doi:10.1074/jbc.270.5.2320

760 62. Chen H, Vermulst M, Wang YE, et al. Mitochondrial fusion is required for mtdna stability in
761 skeletal muscle and tolerance of mtDNA mutations. *Cell*. 2010;141(2):280-289.
762 doi:10.1016/j.cell.2010.02.026

763 63. Yang Y, Ouyang Y, Yang L, et al. Pink1 regulates mitochondrial dynamics through interaction with
764 the fission/fusion machinery. *Proc Natl Acad Sci U S A*. 2008;105(19):7070-7075.
765 doi:10.1073/pnas.0711845105

766 64. Gingras AC, Kennedy SG, O'Leary MA, Sonenberg N, Hay N. 4E-BP1, a repressor of mRNA
767 translation, is phosphorylated and inactivated by the Akt(PKB) signaling pathway. *Genes Dev*.
768 1998;12(4):502-513. doi:10.1101/gad.12.4.502

769 65. Zhang J, Huang L, Shi X, et al. Metformin protects against myocardial ischemia-reperfusion injury
770 and cell pyroptosis via AMPK/NLRP3 inflammasome pathway. *Aging (Albany NY)*.
771 2020;12(23):24270-24287. doi:10.18632/aging.202143

772 66. Techiryan G, Weil BR, Palka BA, Canty JM. Effect of intracoronary metformin on myocardial
773 infarct size in Swine. *Circ Res*. 2018;123(8):986-995. doi:10.1161/CIRCRESAHA.118.313341

774 67. Burkhardt JE, Pandher K, Solter PF, et al. Recommendations for the evaluation of pathology data
775 in nonclinical safety biomarker qualification studies. *Toxicol Pathol*. 2011;39(7):1129-1137.
776 doi:10.1177/0192623311422082

777 68. Moran CM, Thomson AJW. Preclinical Ultrasound Imaging—A Review of Techniques and Imaging
778 Applications. *Front Phys*. 2020;8(May). doi:10.3389/fphy.2020.00124

779 69. Choi YH, Kim SG, Lee MG. Dose-independent pharmacokinetics of metformin in rats: Hepatic and
780 gastrointestinal first-pass effects. *J Pharm Sci*. 2006;95(11):2543-2552. doi:10.1002/jps.20744

781

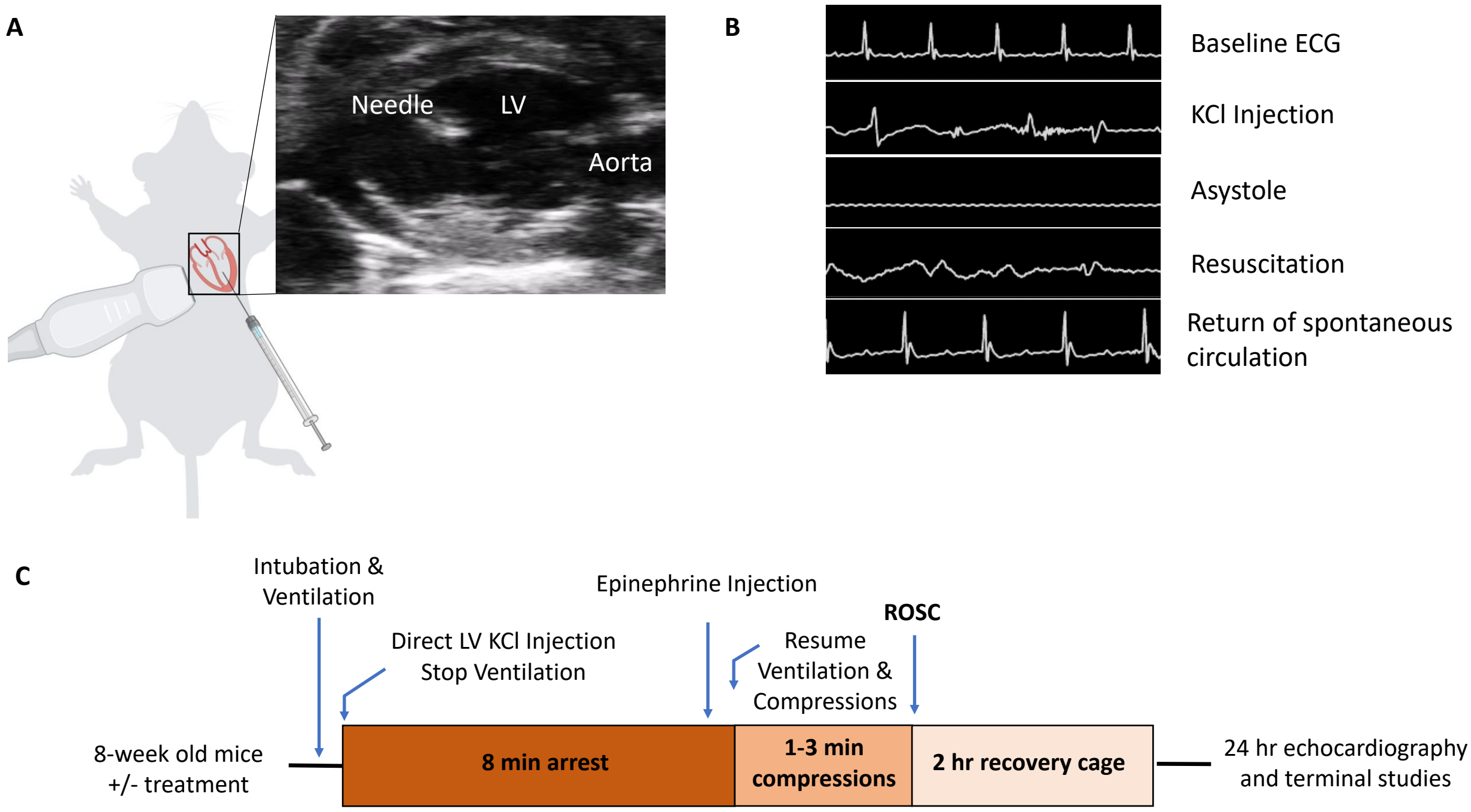

Figure 1. Mouse model of cardiac arrest (CA). A) Cartoon representation of direct left ventricular injection of potassium chloride (KCl) to cause asystole with representative ultrasound image of needle guidance. B) Representative electrocardioagrm (ECG) traces throughout time course of cardiac arrest procedure C) Time course of CA protocol. LV, left ventricle; ROSC, return of spontaneous circulation.

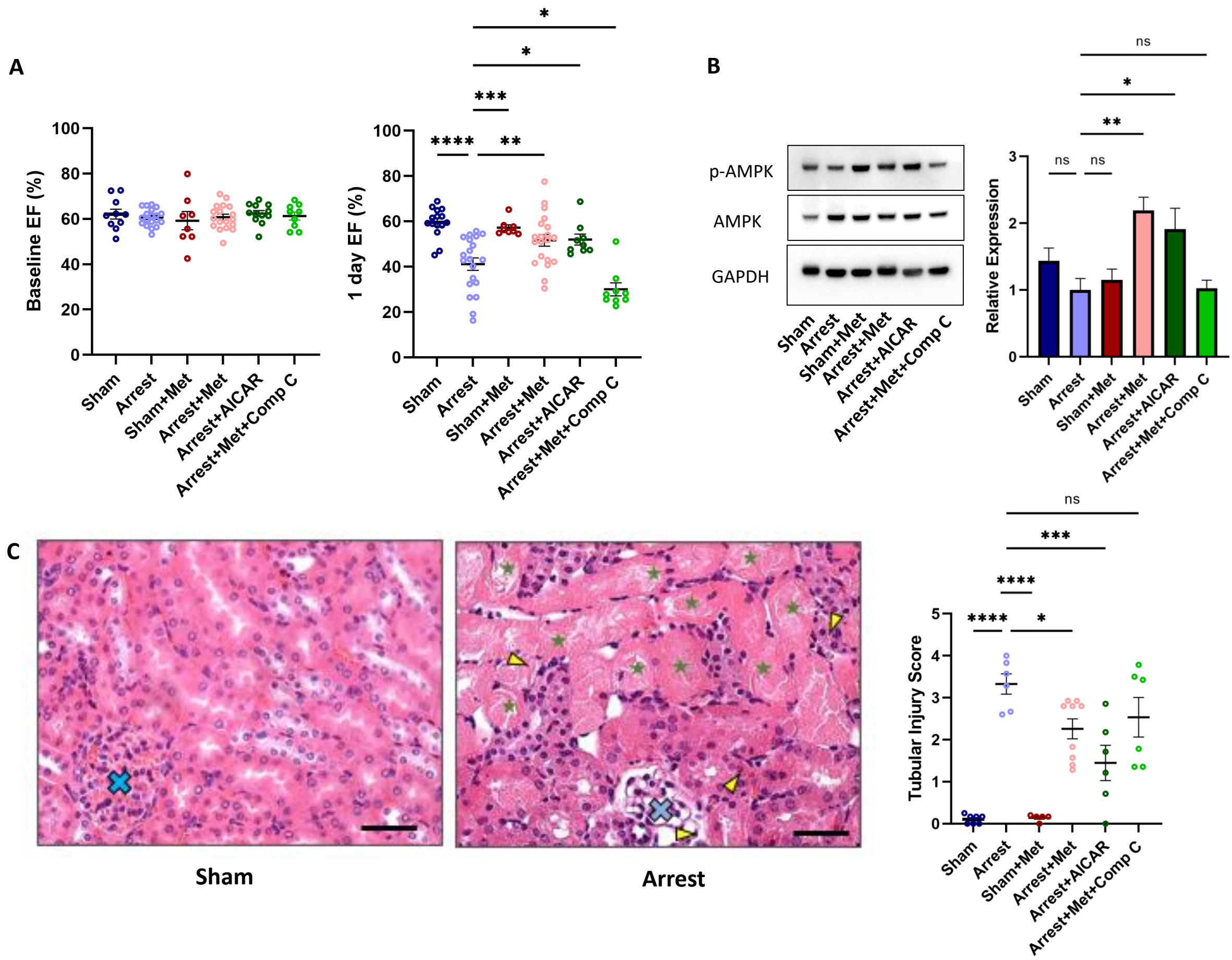

Figure 2. Metformin and AICAR treated mice have improved ejection fraction (EF) , elevated cardiac p-AMPK/AMPK, and less kidney damage than untreated mice one day after cardiac arrest (CA). A) Baseline (left) and one day EF (right) among treatment groups. Circles represent individual mice. B) Representative Western blot analysis of p-AMPK (Thr172), AMPK, and GAPDH for each treatment group and quantification of Western comparing p-AMPK to total AMPK (n=6/group). Full blots are provided in Supplemental Figure 1. C) Representative histologic sections from untreated sham and untreated arrest mice demonstrating proteinaceous casts in renal tubules (green stars) and infiltrates (yellow arrowheads) with glomeruli marked (blue X's). Scale bar = 50 µm) as well as quantification of tubular injury score between groups. Data are expressed as mean ± SEM. P-values: *< 0.05, **< 0.01, ***< 0.001, ****< 0.0001 by one-way ANOVA with Dunnett's multiple comparison test. EF, ejection fraction.

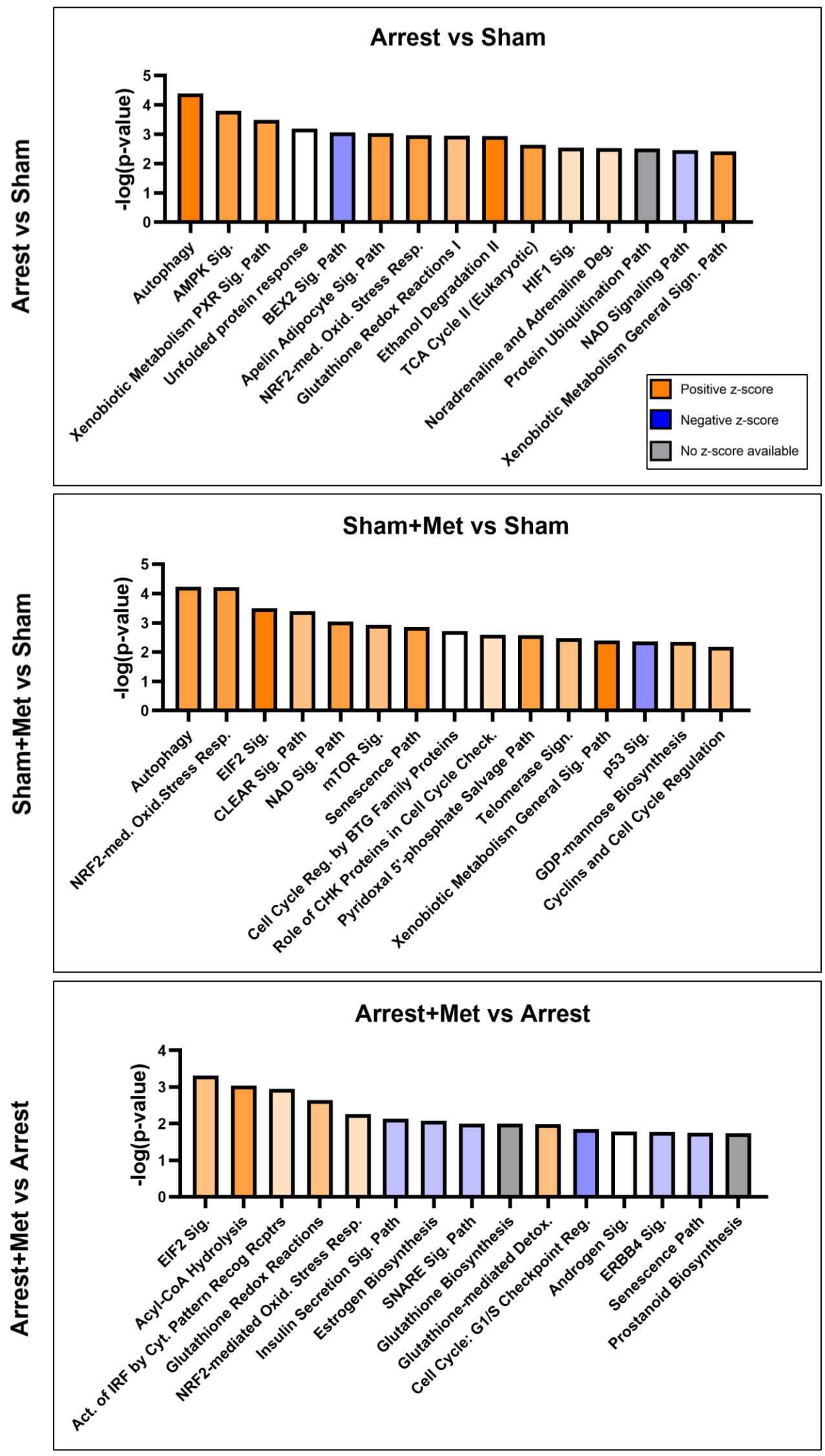

Figure 3. Pathway Analysis Comparing Treatment Groups. Ingenuity Pathway Analysis was used to predict signaling pathways between Arrest and Sham mice (top), Sham+Metformin (Sham+Met) and Sham mice (middle), and Arrest+Metformin (Arrest+Met) to Arrest mice (bottom) based on microarray data collected from left ventricles one day after arrest (n=6/group). Bar-graphs include significance values for pathway changes (-log(p-value)) and are colored according to z-score to predict directionality of changes. Differentially expressed genes were included in the analysis when $p<0.05$ based on microarray data. Principal component analysis and volcano plots are included in Supplemental Figure 2.

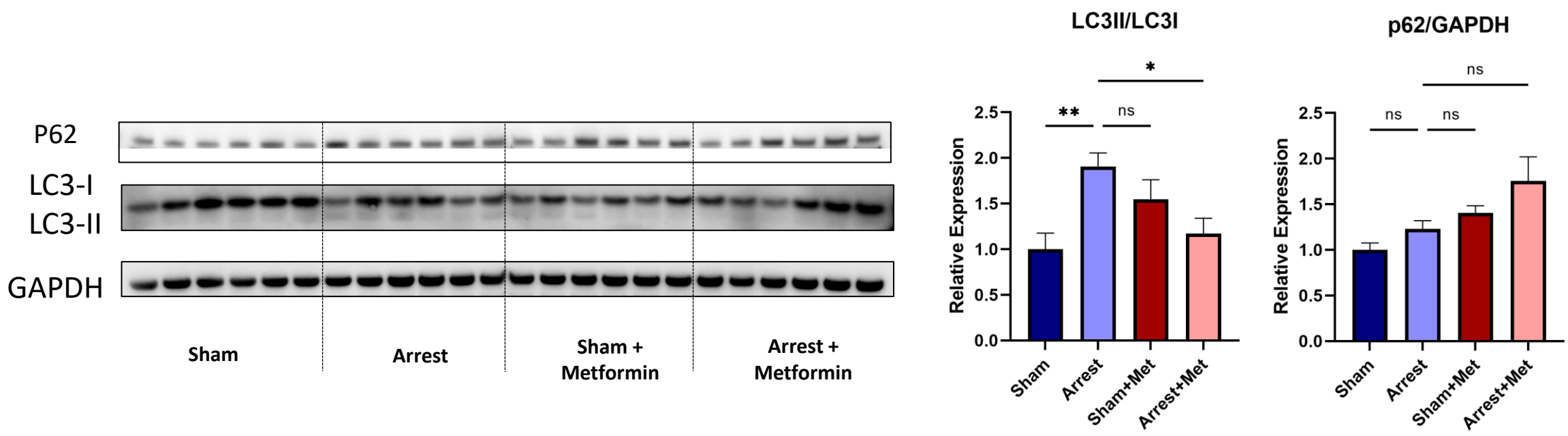

Figure 4. Western Blot Analysis of Autophagy Markers. Western blot images of autophagy-related proteins downstream of AMPK including p62, LC3 (I/II), and housekeeping protein (GAPDH) expression in Sham, Arrest, Sham+Metformin (Sham+Met), and Arrest+Metformin (Arrest+Met) mice (n=6/group). Data are expressed as mean ± SEM. P-values: *< 0.05, **< 0.01 by one-way ANOVA with with Dunnett's multiple comparison.

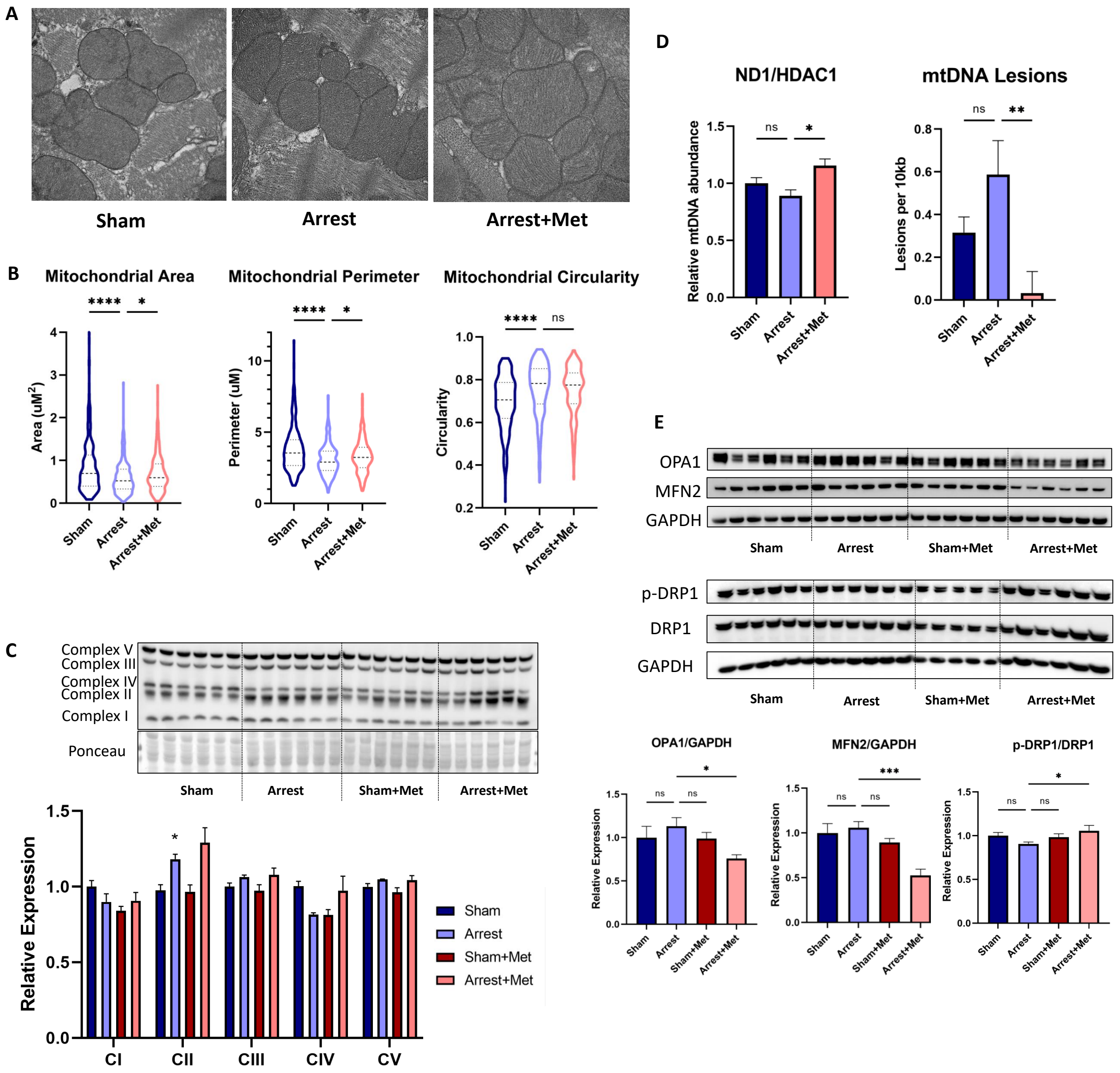

Figure 5. Metformin pretreatment affects mitochondrial size, mtDNA damage, and mitochondrial fission/fusion proteins after cardiac arrest (CA). A) Representative electron microscope images of intrafibrillar mitochondria in Sham, Arrest, and Arrest+Metformin (Arrest+Met) mice one day after surgery (40,000x magnification) B) Violin plot showing mitochondrial perimeter, area, and circularity (n=50 per group). C) Western blot of representative oxidative phosphorylation complex subunits (CI-CV) and bar graph of densitometry (n=6/group, normalized to ponceau stain). Quantitation shown in bar graphs with indicated normalization. D) Bar graph of mtDNA copy number assessment by qPCR quantitation of total DNA preparations of sham (n=5), arrest (n=4), and arrest metformin (n=7) mice. E) Western blot images of markers of mitochondrial fission and fusion (MFN2, OPA1, p-DRP1 (ser616), DRP1) and housekeeping protein (GAPDH) in Sham (n=6), Arrest (n=6), Sham+Met (n=5-6), and Arrest+Met (n=6) mice. B) C). E) Data are expressed as mean ± SEM. P-values: *< 0.05, **< 0.01, ***< 0.001, ***<0.0001 by one-way ANOVA with with Dunnett's multiple comparison. DRP, dynamin-related protein1; MFN2, mitofusin 2; OPA1, dynamin-like 120 kDa protein, mitochondrial.

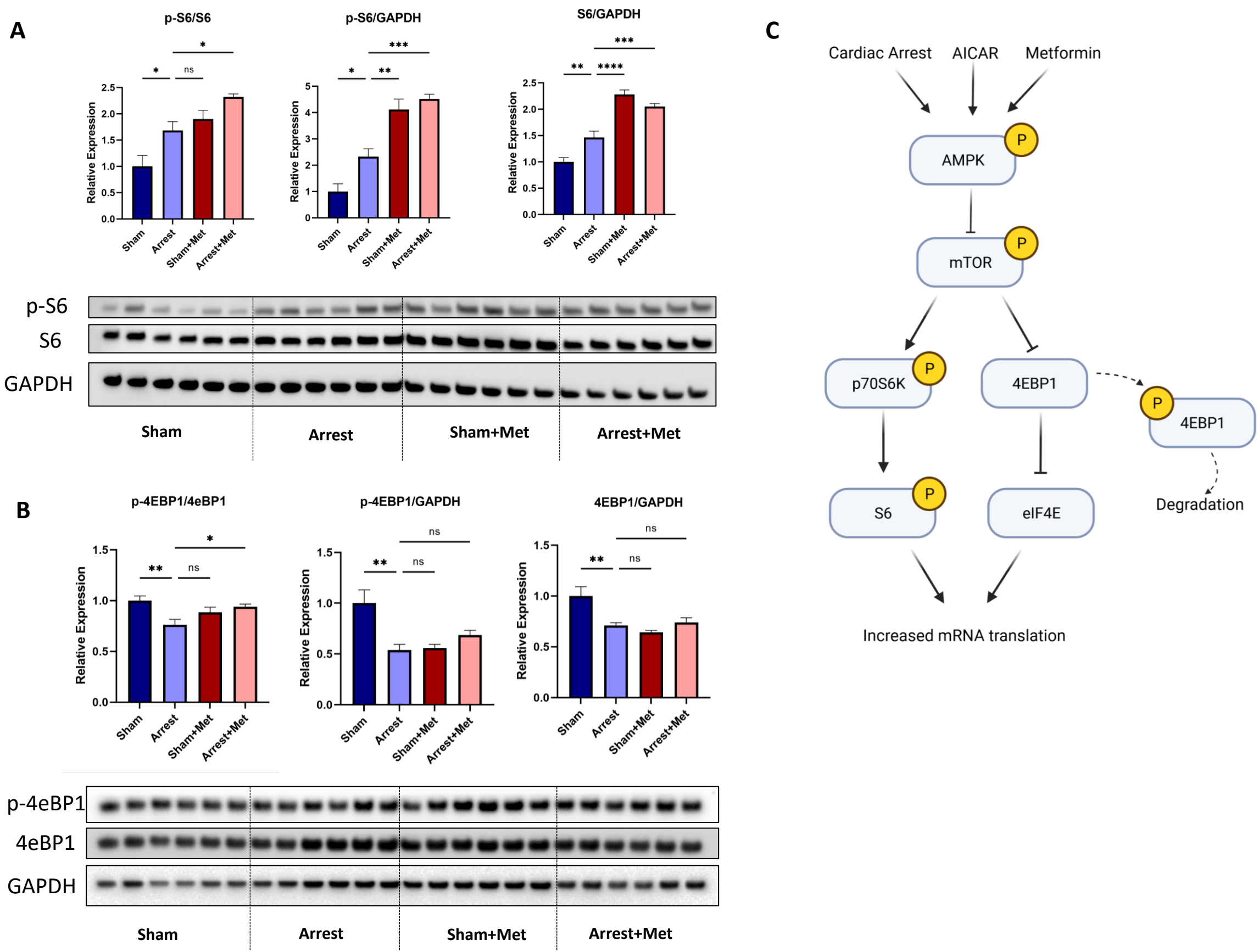

Figure 6. Western Blot Analysis of Protein Synthesis Markers . A) Western blot images of S6 and its phosphorylated form at Ser240/244 and housekeeping protein (GAPDH) expression in Sham, Arrest, Sham+Metformin (Sham+Met), and Arrest+Metformin (Arrest+Met) mice (n=6/group). B) Western blot images of 4eBP1 and its phosphorylated form at Thr37/46 as well as GAPDH. C) Cartoon representation of p-S6 and p-4EBP1 as regulators of mRNA translation downstream of AMPK and mTOR signaling. Data are expressed as mean ± SEM. P-values: *< 0.05, **< 0.01, ***< 0.001 by one-way ANOVA with with Dunnett's multiple comparison test. 4eBP1, eukaryotic translation initiation factor 4e-binding protein 1; mTOR, mechanistic target of rapamycin; S6, ribosomal protein S6.

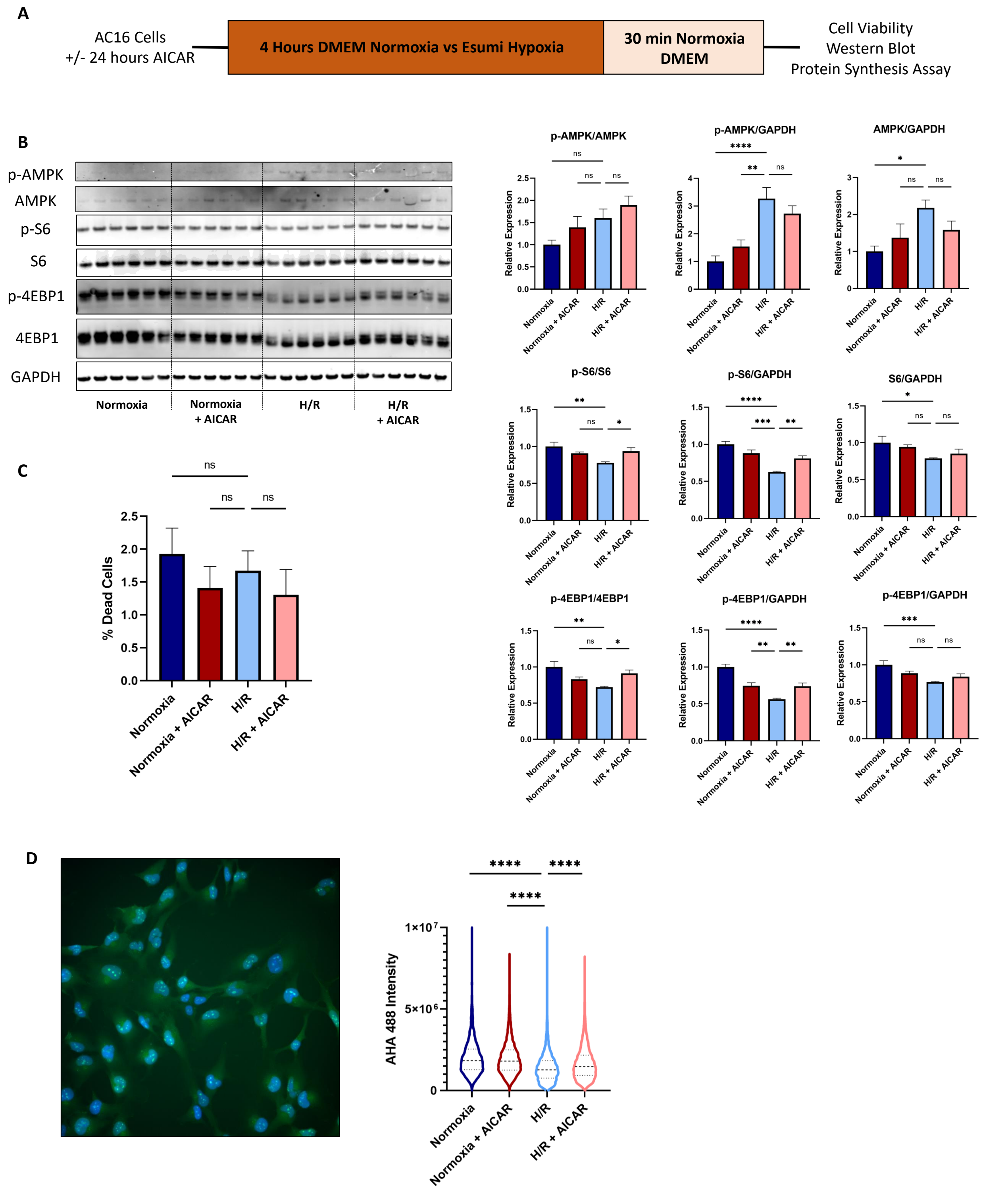

Figure 7. AICAR pretreatment protects against protein synthesis changes in AC16 cells after hypoxia/reoxygenation (H/R). A) Time course of AC16 cells with and without 24 hours of AICAR treatment (1.25 mM). B) Western Blot images of of p-AMPK (Thr172), total AMPK, p-S6 (Ser240/244), total S6, p-4EBP1 (Thr37/46), total 4EBP1, and GAPDH expression from cells 30 min after H/R (n=6/group). C) Quantification of cell death 30-min after H/R. D) Representative image of AHA 488 Protein Synthesis assay demonstrating AHA 488 signal (green) and Hoechst nuclear stain (blue) in AC16 cells 30 min after H/R and quantification of AHA 488 signal intensity surrounding the nuclei after H/R. P-values: *< 0.05, **< 0.01, ***< 0.001 by one-way ANOVA with with Dunnett's multiple comparison test.

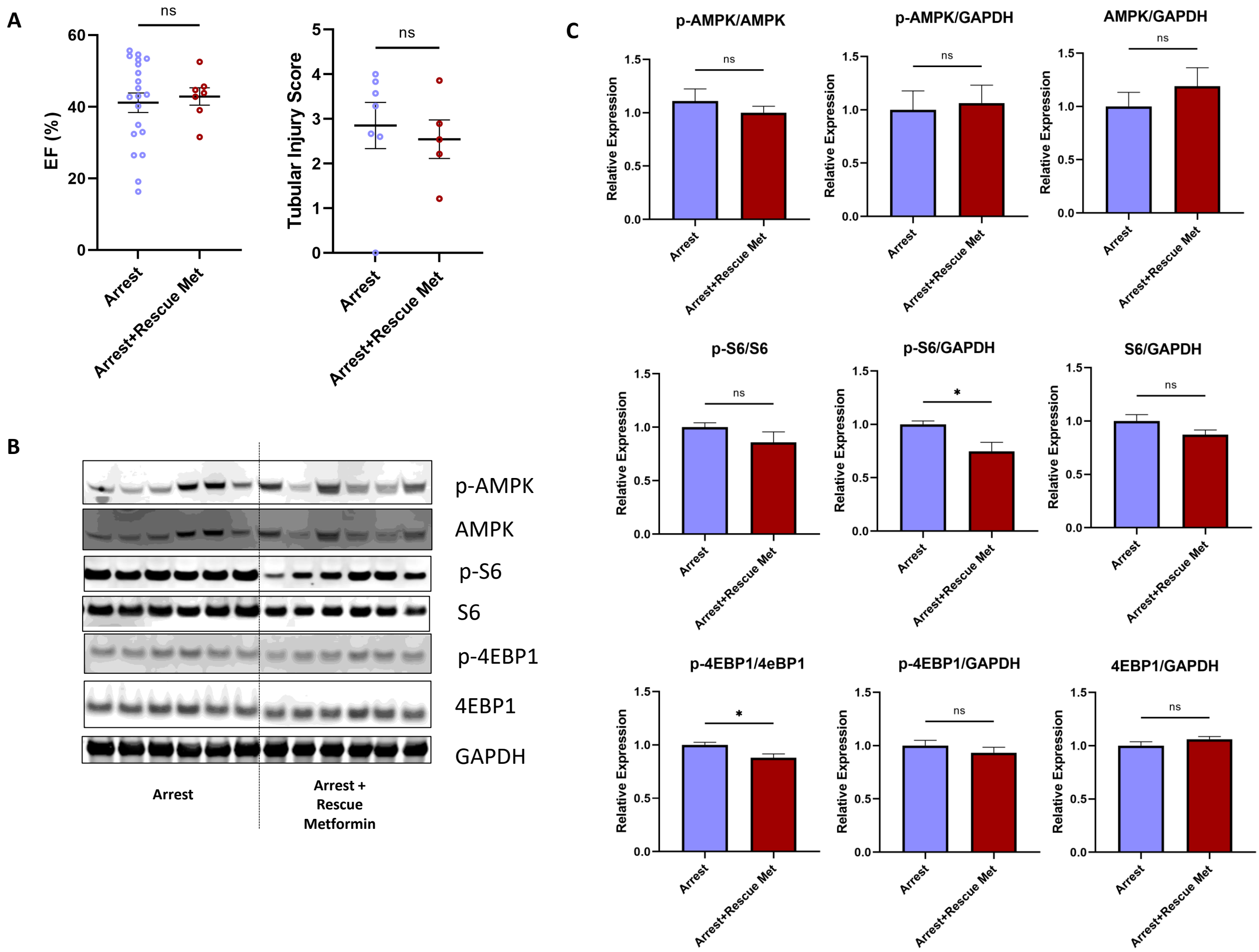

Figure 8. Metformin does not protect cardiac or renal function as a rescue therapy following arrest. A) When given concomitantly with epinephrine, intravenous metformin (rescue met, n=7) did not demonstrate any change to ejection fraction (EF) when compared to untreated arrest mice (n=20; arrest data also presented in Figure 2) or to kidney damage as measured by tubular injury score B) Western Blot images of of p-AMPK (Thr172), total AMPK, p-S6 (Ser240/244), total S6, p-4EBP1 (Thr37/46), total 4EBP1, and GAPDH expression between arrest and arrest + rescue metformin groups (n=6/group) C) Quantification of Western blot changes between groups. *p<0.05 by student's t-test.

Table 1. Surgical data for arrest mice. There are no significant changes to body weight, body temperature at time of extubation, time to return of spontaneous circulation (ROSC), time to extubation, or time to kidney reperfusion between groups when compared to the arrest group. Data are presented as mean ± SEM unless otherwise noted. Statistical comparisons by one-way ANOVA with Dunnett's multiple comparison test.

	Sham (n=20)	Arrest (n=26)	Sham Metformin (n=8)	Arrest Metformin (n=21)	Arrest AICAR (n=9)	Arrest Metformin+ compound C (n=8)
Age (d)	57.55±0.68	57.60±0.59	58.75±0.40	58.80±0.48	58.44±0.50	58.75±0.37
# Female / Total Mice (percentage)	11/20 (55%)	12/26 (46%)	5/8 (63%)	12/21 (57%)	4/9 (44%)	4/8 (50%)
8-wk Body Wt (g)	23.19±0.83	22.97±0.62	21.05±0.88	21.77±0.78	22.59±1.1	22.47±1.23
Temp at Extubation (°C)	35.86±0.15	35.53±0.20	35.96±0.18	35.95±0.12	35.79±0.19	36.21±0.11
ROSC (min)	-	1.31±0.09	-	1.43±0.15	1.44±0.24	1.23±0.12
Time to Extubation (min)	-	22.31±0.66	-	23.64±0.32	22.06±0.90	24.06±0.52
Time to Kidney Reperfusion (min)	-	21.3±0.90	-	21.79±0.57	20.43±1.01	24.70±0.64